



# Location-routing optimization problem for electric vehicle charging stations in an uncertain transportation network: An adaptive co-evolutionary clustering algorithm

Jiabin Wu <sup>a</sup>, Qihang Li <sup>b</sup>, Yiming Bie <sup>c,\*</sup>, Wei Zhou <sup>d</sup>

<sup>a</sup> Business School, Foshan University, Foshan, 528000, China

<sup>b</sup> School of Intelligent Systems Engineering, Sun Yat-sen University, Guangzhou, Guangdong, 510006, China

<sup>c</sup> School of Transportation, Jilin University, Changchun, 130022, China

<sup>d</sup> Department of Civil & Environmental Engineering, National University of Singapore, 117576, Singapore

## ARTICLE INFO

Handling Editor: X Ou

**Keywords:**

Electric vehicles  
Public charging stations  
Location-routing optimization problem  
Intelligent algorithms  
Energy conservation

## ABSTRACT

The rapid growth of Electric Vehicles (EVs) has led to issues such as insufficient and unevenly distributed charging stations, posing an increasingly severe challenge. This not only means higher economic and time costs for EV users traveling to charging stations, but also indicates that EVs need to incur additional energy consumption. To address these challenges, this paper first establishes an extended space-time-state network to describe the temporal variability and uncertainty of the traffic environment. Secondly, considering the impact of the energy consumption incurred by EVs traveling to charging stations (CSs) on the layout of CSs, a co-evolutionary optimization model of the location-routing problem is proposed. To solve the model, a two-stage Adaptive Co-evolutionary Clustering Algorithm (ACECA) integrating an adaptive clustering framework and a co-evolutionary mechanism is designed. Finally, the experiment results indicate that there exists a game between a short-term economic investment and long-term benefits of energy conservation and emission reduction. Moreover, ACECA demonstrates stronger solution performance and robustness compared to other algorithms, with the resulting CS location schemes showing superior advantages in energy conservation and in cost saving for users. The research findings can provide theoretical support for the planning of charging station locations for electric vehicles.

## 1. Introduction

As a representative of the development and application of new energy, electric vehicles (EVs) are favored by governments and consumers around the world for their significant advantages in reducing carbon dioxide (CO<sub>2</sub>) emissions, improving energy efficiency, reducing petroleum dependence, and enhancing passenger experience. As the number of EVs continues to increase, so does the demand for public EV charging stations. Especially in dense cities in Asia, where EV charging at home is often unavailable due to the scarcity of single-family housing resources and personal parking spaces, there is a high reliance on public charging facilities. Therefore, determining the optimal layout of public charging stations for electric vehicles is a crucial research topic to effectively meet the charging demand of EVs and alleviate range anxiety caused by low battery capacity.

The quantity and distribution of public charging stations are vital factors affecting the development of the electric vehicle industry, which is closely related to the EV user experience and the long-term benefits of charging station operators. Many researchers have studied the charging station layout problem for different types of EVs, including cabs [1–3], electric buses [4], and private EVs, and have achieved significant and meaningful results. However, the existing literature still reveals some research gaps. Firstly, most studies utilize Euclidean distance to describe the travel costs between demand points and charging stations and build the EV charging station (EVCS) location optimization models, ignoring the long-term impact of optimal path decisions for EVs traveling to charging stations on the layout of CSs. Secondly, while most studies have considered factors such as economic costs and user demand, few studies analyze the additional energy consumption generated by EVCS location from the perspective of environmental benefits. Finally, although

\* Corresponding author.

E-mail address: [yimingbie@126.com](mailto:yimingbie@126.com) (Y. Bie).

existent studies have considered the spatiotemporal characteristics of existing or future charging demand under static transportation networks, they have neglected the impact of random fluctuations in travel time to charge on the degree of user capture at charging stations and thus on the CS layout.

To address these aforementioned shortcomings, this paper proposes a co-evolutionary optimization model of location-routing problem (CEOLRP), taking into account the uncertainty of the traffic environment of the road network and the impact of the energy consumption generated by the EV traveling to the CS on the CS location layout. A two-stage Adaptive co-evolutionary clustering algorithm (ACECA) is then designed to solve the model.

The main contributions of this paper are the following. (i) An extended space-time-state network is designed to describe parameters in dimensions including time, location, and battery status during EV operation in the road network. Based on this, the impact of the EV path decision to the CS on the CS location scheme is considered. A co-evolutionary optimization model of CS location and EV routing problem is then constructed. (ii) In the model construction, the effects of uncertainty of traffic environment, signal control and other factors on EV travel time and energy consumption are taken into account, which helps reduce the long-term environmental pollution indirectly caused by CS location, enhance the convenience of EV charging. (iii) A novel two-stage ACECA is designed based on the adaptive clustering framework and co-evolutionary mechanism. By efficiently jointly solving the CS location and EV routing problem, this algorithm can obtain CS location schemes with higher economic and environmental benefits. (iv) The impact of traffic network uncertainty, road network scale, traffic volume, and charging station capacity on the model results is analyzed, and the influence on the practical application scenarios, political implications, and economic benefits of this study is discussed.

The rest of this paper is organized as follows. In Section 2, we review the literature on factors influencing charging station layout, model construction, and solution algorithms. In Section 3, a co-evolutionary optimization model of location-routing problem is developed based on an extended space-time-state network and. In Section 4, we propose a two-stage adaptive co-evolutionary clustering algorithm. The basic principles and steps of the proposed algorithm are presented. In Section 5, we carry out case studies and conduct algorithm simulation experiment. Section 6 summarizes the study and provides prospects for future research.

## 2. Literature review

The research on EVCS location-routing can be summarized from three main aspects: differences in influencing factors, variations in model optimization objectives, and distinctions in solving algorithms.

### 2.1. Influencing factors

The study of factors influencing the charging station location is crucial for the rational planning of charging station networks. The traffic flow and charging demand are the most important influencing factors for EVCS location selection in the transportation network [5,6]. However, due to the limitations of the popularity of measurement equipment, measurement stability, and data confidentiality, it is difficult to obtain sufficiently reliable traffic flow and charging demand data. Considering the correlation between traffic data and electric vehicle travel and charging behavior, some works indirectly predict charging demand and load by establishing electric vehicle user equilibrium models to predict traffic flow [7,8]. Previous studies to achieve prediction for EV charging load has mainly consisted of model-based methods and data-driven methods. In particular, according to types of user behavior data, the data-driven methods are further divided into result-data-driven and process-data-driven approaches [9,10]. In addition, with the popularity of smartphones, several transportation network

companies have developed smartphone-based ridesharing systems. The emerging ridesharing platforms are becoming the main market for electric vehicles, which will not only significantly change travelers' mode and route choice behavior, but also reshape the spatial distribution of traffic flows and charging load of electric vehicles within the network [11–13]. Therefore, the effectiveness of solving the ridesharing user equilibrium problem may affect the optimal locations of EVCSs [14].

Other influencing factors of CS location include population density, urban planning, and building layout. For instance, Guo et al. examined the impact of range anxiety, service level, and heterogeneous user perception on charging station layout [15]. Hu et al. explored the effects of charging anxiety on CS location, considering cruising time, queuing time, and charging duration of EV charging process [16]. Erbaş et al. identified fifteen influencing factors from various perspectives, and proposed a GIS-based multi-criteria decision analysis method [17]. Liu et al. examined the impact of charging satisfaction and distributed renewable energy integration on charging station location [18]. Panah et al. investigated the impact of stakeholders, municipalities, and electricity distribution companies on charging station location [19]. Guler et al. proposed a CS location method combining GIS with a multi-criteria decision-making approach [20]. Rani et al. proposed an integrated Fermatean fuzzy MULTIMOORA approach to identify the quantitative and qualitative influencing factors of CS location [21]. Zhou et al. proposed a location and sizing decision-makings model for fast charging station planning problem in electrified transportation networks, considering the EV self-serving routing and charging behaviors [22]. Song et al. jointly locates charging stations and segments in the space-time-electricity network by maximizing the accessibility of electric vehicles [23]. Wang et al. proposed an optimization model for charging station planning considering the spatio-temporal characteristics of EV charging demand [24].

Previous studies have explored the primary influencing factors of CS locating, providing valuable theoretical guidance for subsequent research. However, research on the impact of future traffic network uncertainty, traffic flow, and grid capacity on the planning of charging station siting is relatively scarce and requires further exploration.

### 2.2. Model construction

In the modeling process of Electric Vehicle Charging Stations (EVCS), factors such as operating costs, charging demand, distance, coverage, and power supply capacity need to be taken into account in order to scientifically plan the CS location and ensure the efficiency and sustainability of CS network. Zhou et al. constructed an optimal distribution model of EVCS from the perspective of total social cost [25]. He et al. incorporated supply-demand constraints as well as policy and spatial constraints to build a contextualized EVCS optimization model [26]. Ren et al. quantified qualitative indicators and established a charging station location optimization model minimizing the total social cost [27]. Hosseini et al. constructed a Bayesian network model incorporating quantitative and subjective factors by considering uncertainty, qualitative, and quantitative factors in the evaluation of location schemes [28]. Li et al. studied a microgrid composed of wind and photovoltaics, EVCS, and energy storage system, and proposed a robust optimization model for distributed charging station location based on the combination of the road network and the power grid [29]. There exists a high degree of autonomy of EV users in charging behavior, which makes it difficult to achieve consensus in balancing the interrelated interests of investors and users. Li et al. proposed a bi-level programming model to balance the interests of investors and EV users and optimize the overall economic cost [30]. Since the location cost and operational benefits of charging stations vary with time, location and capacity, some scholars have considered the time-varying characteristics of EV charging demand and electricity tariffs. Li et al. obtained the spatiotemporal distribution of electric taxi charging demand by accurately modeling the driving and

charging behaviors of electric taxis for joint modeling of user behavioral decisions and charging station planning [31]. Qiao et al. proposed a two-phase approach consisting of data processing and model optimization, and developed a spatiotemporal mathematical programming model with equilibrium constraints to minimize social costs [32]. Song et al. focused on the spatiotemporal power accessibility of electric vehicles and constructed a three-dimensional space-time-power network integer programming model [33].

These studies considered users' charging demands and behavioral characteristics, aiming to construct multi-objective mathematical models to reduce societal costs or enhance the economic benefits of operators and user experiences. However, there is still significant room for further research in minimizing additional travel energy consumption resulting from EVCS siting from an energy-saving perspective.

### 2.3. Model solving algorithms

Algorithms related to optimal location models play a crucial role in the research of charging station location, because such algorithms can efficiently handle large amounts of spatial and data information to identify the optimal location solution [34–36]. In terms of heuristic algorithms, Li et al. proposed a two-phase heuristic approach combining a two-layer genetic algorithm and simulated annealing to solve the public charging station localization and route planning problem of electric vehicles [37]. Jordán et al. employed a genetic algorithm to optimize the possible locations of charging stations for the electric vehicles [38]. Li et al. proposed a multi-swarm genetic algorithm with an improved crossover operator to optimize the construction cost of CS and the travel cost of EV users [39]. Wang et al. designed a neighborhood mutation immune clonal selection algorithm (neighborhood mutation immune clonal selection algorithm) to determine the location and scale of charging stations from the perspective of minimizing annual CS costs [40]. Altundogan et al. proposed a graph-based genetic algorithm to solve the CS location problem given a specific number of charging stations in the city [41]. Hu et al. designed a heuristic algorithm incorporating a greedy algorithm, a greedy alternative algorithm, and a bi-level genetic algorithm to maximize EV charging service satisfaction [16]. With respect to exact algorithms, Song et al. developed a Benders decomposition method with a stable technique to maximize the spatiotemporal power accessibility of EV users [42]. Wei et al. proposed a solution method for EVCS location in a large urban road network by combining a multi-criteria decision model and segment matching technique based on the multi-layer road index system [43]. Furthermore, some researchers have addressed the EVCS location problem using machine learning techniques. For example, Zhao et al. developed a formula describing finite discrete Markov decision process in a reinforcement learning framework to solve the optimal deployment problem of electric vehicle charging stations on traffic and power distribution networks [44]. Li et al. trained the optimal pricing strategy of EVCS using reinforcement learning algorithm based on a three-layer location selection model with dynamic pricing to maximize cumulative benefits [45].

Previous studies have established a rich body of optimization theory and solution algorithms, which hold significant theoretical and practical value. However, there is a lack of research focusing on the integrated adaptive clustering framework and cooperative evolution mechanism for the CS location-routing combination optimization problem. Developing a two-stage solution algorithm that incorporates these elements could rapidly generate high-quality solutions.

## 3. Model formulation

### 3.1. Problem statement and notations

This study focuses on the location problem for public charging stations catering to all private EVs. Charging stations are typically installed

in travel destinations such as shopping centers, workplaces, and homes, with less impact on public facilities and power supply systems. The optimization of such CS location schemes is more flexible and can be done without considering the given prebuilt location constraints. Furthermore, EV drivers primarily select charging stations based on the driving distance and travel time along the navigation route (the actual shortest path), rather than the straight-line distance. In summary, this study is to jointly solve the CS location problem and the EV charging routing problem based on long-term predicted traffic flow, taking into account the spatiotemporal distribution of charging demand, uncertain travel time, and limited service range, in order to find the optimal location for CSs and minimize the CS construction cost, user travel cost, and energy waste. The parameters and variables in this model are presented in Appendix A.

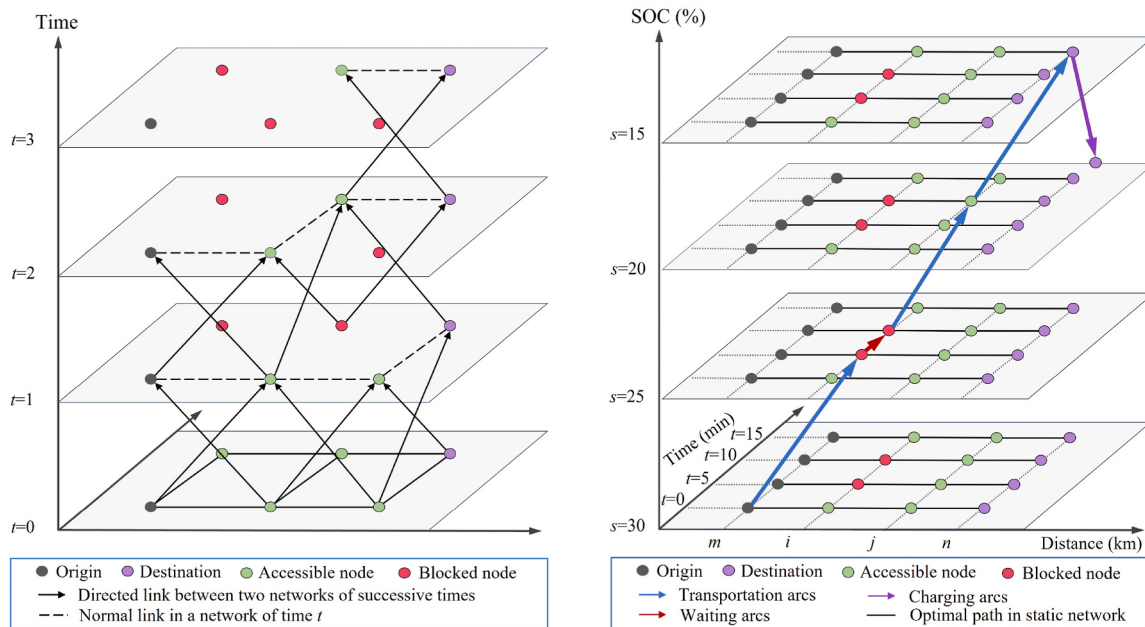
### 3.2. Illustration of the extended space-time-state network

Assuming the spatiotemporal distribution of charging demand is known, let the set of EV charging demand points be  $M$ , which includes  $N_m$  demand points. Any demand point  $m$  belongs to  $M$ , where the planned EV charging time for each demand is not the same. The set of potential CS locations is denoted as  $N$ , which includes  $N_n$  charging stations locations, and any location  $n$  belongs to  $N$ . Using a bipartite graph  $G = (V, A)$  to represent the topology of the road network, which includes several nodes and edges, where nodes  $i, j \in V$ , and edge  $(i, j) \in A$ . Owing to factors such as signal control facilities, road construction, and traffic accidents, node connectivity undergoes changes, resulting in two states: "accessible" and "blocked", fluctuating over time. The changes in node connectivity in the road network are illustrated in Fig. 1 (a).

In a given time range  $T$  and a limited EV battery energy state  $S$ , the road network structure diagram  $G = (V, A)$  can be extended to a space-time-state network composed of several spatiotemporal state vertices  $\bar{V}$  and spatiotemporal state edges  $\bar{A}$ . In the space-time-state network, any node  $(i, t, s) \in \bar{V}$  represents the position, time, and battery state. Any edge  $(i, j, t, t', s, s') \in \bar{A}$  represents a directed journey from physical node  $i$  to node  $j$  departing at time  $t$  and arriving at time  $t'$  with battery state-of-charge (SOC) changing from  $s$  to  $s'$ . The SOC dimension can describe not only the discharge process of the EV as it goes to the charging station, but also its charging process at the charging station.

The process of an EV traveling from a demand point to a charging station is illustrated in Fig. 1(b). In this depiction, the spatiotemporal state network comprises three types of multidimensional edges, which are specified as follows.

- (1) Transportation arcs. Transportation arc  $(i, j, t, t + T_{ijt}, s, s - e_{ijt})$  contains the travel time  $T_{ijt}$  and energy consumption  $e_{ijt}$  of an EV traversing this arc at time  $t$ , where the travel time and energy consumption of an EV journey from node  $i$  to  $j$  at time  $t$  are closely related to its departure time.
- (2) Waiting arcs. Waiting arc  $(i, i, t, t + 1, s, s' = s)$  include the waiting cost per unit time for an EV at node  $i$ . The cost is approximately considered as 0 when the EV is waiting at a signalized intersection.
- (3) Charging arcs. Charging arc  $(n, n, t, t'' = t + T_{mn}^{\text{char}}, s, s' = s + E_{mnt})$  involve the charging quantity  $E_{mnt}$  and charging time  $T_{mn}^{\text{char}}$  for an EV charging at charging station  $n$  until reaching the initial battery state  $s_m$ , where,  $E_{mnt}$  represents the total energy consumption of an EV journey from demand point  $m$  to charging station  $n$  at time  $t$ , indirectly reflecting the carbon emissions and environmental pollution associated with the charging station location scheme.



(a) The evolution process of connectivity state in the spatiotemporal network  
(b) The process of EV going to charging stations in the time-space-state network

**Fig. 1.** An example of the extended time-space-state network.

### 3.3. Dynamic stochastic characteristics of an extended space-time-state network

#### 3.3.1. Total route travel time

Due to the influence of the time-varying and uncertain nature of road traffic conditions, the travel time in links  $T_{ijt}$  exhibits significant dynamic and random features. Therefore, this paper employs the BPR function [46] to represent the travel time  $T_{ijt}$  of EV in link  $(i, j)$  at time  $t$ , formulated as follows:

$$T_{ijt} = T_{ijt}(Q_{ijt}, C_{ijt}) = a_{ijt} \left( 1 + \beta \left( \frac{Q_{ijt}}{C_{ijt}} \right)^{\gamma} \right) \quad (1)$$

where  $a_{ijt}$ ,  $Q_{ijt}$ , and  $C_{ijt}$  represent the travel time, free-flow travel time, traffic flow, and capacity in link  $(i, j)$  at time  $t$ , respectively.  $\beta$  and  $\gamma$  are parameters.

Assuming the independence of travel times for different road links, the total travel time for an EV traveling from demand point  $m$  to alternative charging station  $n$  at time  $t$  can be expressed as:

$$T_{mnt} = \sum_{(i,j) \in P_{mn}} T_{ijt} = \sum_{(i,j) \in P_{mn}} a_{ijt} \left( 1 + \beta \left( \frac{Q_{ijt}}{C_{ijt}} \right)^{\gamma} \right) \quad (2)$$

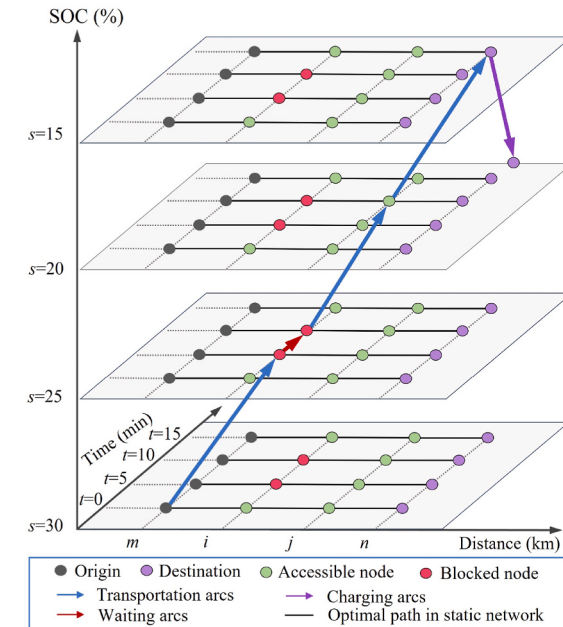
where  $P_{mn}$  represents the shortest path from demand point  $m$  to charging station  $n$ , consisting of various nodes  $i, j$  and edges  $(i, j) \in P_{mn}$ .

#### 3.3.2. Path travel time budget

The path travel time budget is the sum of a traveler's expected travel time and the safety time reserved to ensure timely arrival at the destination. When the travel time in road links follows a normal distribution, the travel time budget for a road link  $(i, j)$  at time  $t$ , at a confidence level  $\alpha$ , can be represented as:

$$\hat{T}_{ijt} = \mu_{ijt} + \sigma_{ijt} \Phi^{-1}(\alpha) \quad (3)$$

where  $\hat{T}_{ijt}$ ,  $\mu_{ijt}$ , and  $\sigma_{ijt}$  represent the travel time budget, mean, and standard deviation of EV traveling through link  $(i, j)$  at time  $t$ , respectively.  $\Phi^{-1}(\cdot)$  is the inverse function of the standard normal distribution.



From equation (3), it can be inferred that the travel time budget is related to the mean, variance, confidence level, and the distribution it follows. Thus, the total travel time budget for a path can be expressed as:

$$\hat{T}_{mnt} \approx \mu_{mnt} + \sigma_{mnt} \Omega(\alpha) \quad (4)$$

where  $\hat{T}_{mnt}$  represents the total travel time budget for an EV traveling from demand point  $m$  to charging station  $n$  at time  $t$ .  $\mu_{mnt}$ ,  $\sigma_{mnt}$ , and  $\Omega(\cdot)$  denote the mean, and variance of the total travel time, and the distribution it follows, respectively.

Based on the research findings by Xu et al. [47],  $\Omega(\cdot)$  is related to the skewness and kurtosis of the total travel time, expressed as:

$$\begin{aligned} \Omega(\alpha) = & \Phi^{-1}(\alpha) + \frac{1}{6} \left[ (\Phi^{-1}(\alpha))^2 - 1 \right] S_{mnt} + \frac{1}{24} \left[ (\Phi^{-1}(\alpha))^3 - 3\Phi^{-1}(\alpha) \right] K_{mnt} \\ & - \frac{1}{36} \left[ 2(\Phi^{-1}(\alpha))^3 - 5\Phi^{-1}(\alpha) \right] S_{mnt}^2 \end{aligned} \quad (5)$$

where  $S_{mnt}$  and  $K_{mnt}$  represent the skewness and kurtosis of the total travel time, respectively.

#### 3.3.3. Reliability of total path travel time

The reliability of the total path travel time  $R_{mnt}$  is defined as the probability that the actual travel time used by the EV from demand point  $m$  along path  $P_{mn}$  to charging station  $n$  at time  $t$  is less than or equal to the travel time budget, expressed as follows:

$$R_{mnt} = P\{T_{mnt} \leq \hat{T}_{mnt}\} \quad (6)$$

If the probability density distribution function of the total path travel time  $\Omega(\cdot)$  and the total travel time budget  $\hat{T}_{mnt}$  are known, the reliability  $R_{mnt}$  can be calculated. To validate the model results, assuming  $T_{mnt}$  follows a normal distribution,  $R_{mnt}$  can be formulated as follows:

$$R_{mnt} = \Phi \left( \frac{\hat{T}_{mnt} - \mu_{mnt}}{\sigma_{mnt}} \right) \quad (7)$$

From equation (4), it can be inferred that:

$$\Omega(\alpha) \approx \frac{\widehat{T}_{mn} - \mu_{mn}}{\sigma_{mn}} \quad (8)$$

The proposed model adopts the value of the total travel time reliability at 85 % ( $R_{mn}^t = 85\%$ ) as the shortest travel time between two nodes. In other words, the travel time is set to  $T_{mn}$  when the reliability of the travel time of the path from the demand point  $m$  to the charging station  $n$  is 85 %.

### 3.4. EV energy consumption estimation model considering dynamic stochastic speed

Signal control facilities significantly impact EV energy consumption. This paper assumes that the energy consumption of EV traveling through nodes such as non-signalized intersections, merging zones, and diverging zones is similar to that on basic road links. Therefore, the total energy consumption for an EV traveling from demand point  $m$  to charging station  $n$  at time  $t$ ,  $E_{mn}$ , is primarily composed of energy consumption in road links and at signalized intersections, expressed as:

$$E_{mn} = E_{mn}^{\text{link}} + E_{mn}^{\text{node}} \quad (9)$$

where  $E_{mn}^{\text{link}}$  and  $E_{mn}^{\text{node}}$  represent the energy consumption in road links and at signalized intersections for an EV traveling from demand point  $m$  to charging station  $n$  at time  $t$ , respectively.

#### 3.4.1. EV energy consumption estimation in road links

The EV energy consumption in road links is influenced by various factors such as air conditioning consumption, the space mean speed in segments, and the road slope [48]. Therefore, the energy consumption  $E_{mn}^{\text{link}}$  for an EV traveling from demand point  $m$  to charging station  $n$  at time  $t$  in a road segment can be expressed as:

$$E_{mn}^{\text{link}} = E_{mn}^{\text{drive}} + E_h^{\text{air}} \cdot L_{mn} \quad (10)$$

where  $E_{mn}^{\text{drive}}$  denotes the energy consumption of EV traveling from demand point  $m$  to charging station  $n$  in road segments at time  $t$ .  $E_h^{\text{air}}$  is the average air conditioning energy consumption per kilometer for EV at an ambient temperature of  $h$ .  $L_{mn}$  is the length of the shortest path from demand point  $m$  to charging station  $n$ .

The total energy consumption for EV in road segments can be represented as:

$$E_{mn}^{\text{drive}} = \sum_{(i,j) \in P_{mn}} (f_{ijt} \cdot l_{ij} \cdot y_{ij}) \quad (11)$$

where  $y_{ij}$  is a binary decision variable indicating whether EV passes through segment  $(i, j)$ . The variable takes value 1 if the vehicle passes through segment  $(i, j)$ ; otherwise, it takes value 0.  $f_{ijt}$  is the total force acting on EV when it travels through segment  $(i, j)$  at time  $t$ .  $l_{ij}$  denotes the length of segment  $(i, j)$ .

When EV travels uphill, i.e.  $\theta_{ij} \leq 90^\circ$ , the vehicle needs to overcome the climbing resistance  $f_{ijt}^g$ . When the vehicle travels downhill, i.e.  $\theta_{ij} > 90^\circ$ , the gravitational force works together with the tractive force of the vehicle. Therefore,  $f_{ijt}$  can be expressed as:

$$f_{ijt} = \begin{cases} f_{ijt}^* + f_{ijt}^g, & \theta_{ij} \leq 90^\circ \\ f_{ijt}^* - f_{ijt}^g, & \theta_{ij} > 90^\circ \end{cases} \quad (12)$$

$$f_{ijt}^g = mg \sin \theta_{ij} \quad (13)$$

The tractive force is approximated as:

$$f_{ijt}^* = a_1 \bar{v}_t^2(i, j) - f_{ijt}^r mg \cos \theta_{ij} \quad (14)$$

where  $f_{ijt}^*$  represents the tractive force of EV traveling on segment  $(i, j)$  at

time  $t$ .  $f_{ijt}^g$  denotes the climbing resistance for EV passing through segment  $(i, j)$ .  $a_1$  is a vehicle-specific parameter obtained by the regression model.  $\bar{v}_t(i, j)$  is the space mean speed in segment  $(i, j)$  at time  $t$ .  $f_{ijt}^r$  denotes the rolling resistance coefficient of EV traveling in segment  $(i, j)$  at time  $t$ , related to the average speed and can be expressed as a linear function  $f_{ijt}^r = \eta_1 + \eta_2 \cdot \bar{v}_t(i, j)$ , where  $\eta_1$  and  $\eta_2$  are parameters of the rolling resistance coefficient, values for which can be referred to Ref. [38].  $\theta_{ij}$  represents the angle between segment  $(i, j)$  and the horizontal direction, namely the road slope angle.  $m$  is the weight of the vehicle.  $g$  is the gravitational constant.

As the primary equipment for energy consumption of EV accessories, the onboard air conditioner's energy consumption is significantly affected by external environmental temperature, directly impacting the total energy consumption of the EV [49]. Under the same environmental temperature, the air conditioning energy consumption of the same EV model is also influenced by factors such as the driver's driving habits, vehicle condition, and travel segments. Therefore, this paper uses the average consumption per hundred kilometers to describe the impact of environmental temperature on EV air-conditioning energy consumption.

$$E_h^{\text{air}} = \begin{cases} \frac{E_h}{100}, & \text{If the air conditioning is turned on} \\ 0, & \text{Otherwise} \end{cases} \quad (15)$$

where  $E_h$  represents the air conditioning consumption per hundred kilometers for EV at an environmental temperature of  $h$ .

#### 3.4.2. EV energy consumption estimation at signalized intersections

When an EV enters the range of a signalized intersection, it typically decelerates, comes to a stop, waits, and then accelerates to cross the intersection.  $t_k$  denotes the moment when EV arrives at node  $k$  (signalized intersection).  $[t_k, t_{k1}]$  represents the uniform deceleration process of the vehicle until it stops.  $(t_{k1}, t_{k2})$  represents the waiting process at node  $k$ .  $(t_{k2}, t_{k3})$  represents the uniform acceleration process. The energy consumption for EV passing through node  $k$  is given by:

$$E_{mn}^{\text{node}} = \sum_{k \in P_{mn}} E_k(t_k), t_k \in [t, t + T_{mn}] \quad (16)$$

$$E_k(t_k) = E_r + \int_{t_k}^{t_{k3}} W_e(t) dt + \int_{t_{k2}}^{t_{k3}} [W_t(t) + W_a(t)] dt \quad (17)$$

where  $E_k(t_k)$  denotes the energy consumption when EV passes through node  $k$  at time  $t_k$ .  $E_r$  represents the energy consumption recovered during the braking process.  $W_t$ ,  $W_a$ , and  $W_e$  stand for the power consumed by EV in overcoming resistance, accelerating, and operating vehicle auxiliary devices during the travel through node  $k$ , respectively.

The energy recovered during braking [50] is given by:

$$E_r = \lambda \eta_c \left[ E_b - \sum_{u \in U} (F_r + F_d + F_j) v_b dt \right] \quad (18)$$

where  $E_b$  stands for the energy consumed by vehicle braking.  $U$  and  $u$  represent the total number and ordinal number of braking time intervals under EV driving conditions, respectively.  $\lambda$  is the percentage of motor braking force to the total braking force.  $\eta_c$  represents the efficiency of the flywheel inertia charging the battery via the electric motor.  $v_b$  denotes the speed of the vehicle under braking.  $F_r$ ,  $F_d$ , and  $F_j$  represent the rolling resistance, air resistance, and acceleration resistance of the EV, respectively.

The energy consumption during braking is given by:

$$E_b = \left( \frac{1}{3.6} \right)^2 \times \frac{1}{10^3} \frac{1}{2\eta_{EV}} \sum_{u \in U} m(v'_u - v_u^2) \quad (19)$$

where  $\eta_{EV}$  is the overall efficiency of the vehicle.  $v'_u$  and  $v_u$  represent the final and initial speeds of the vehicle in the  $u$ -th braking time interval, respectively.

When the EV starts accelerating from a parked state and passes through a signalized intersection, ignoring the influence of slope, the instantaneous power consumed for acceleration and overcoming resistance (air resistance and frictional resistance) can be calculated as follows.

$$W_t = v_t \left( mgf_r + \frac{f_d A \chi \rho v_t^2}{2} \right) \quad (20)$$

$$W_a = \delta m \frac{dv_t}{dt} \quad (21)$$

where  $v_t$  denotes the speed of EV at time  $t$ .  $\delta$  is the rotating mass conversion factor.  $f_d$  is the air resistance coefficient.  $\chi$  stands for the vehicle frontal area.  $\rho$  is the air density.  $f_r$  represents the rolling coefficient for the vehicle traveling through the intersection.

### 3.5. Objective function

In general, the construction of EV charging stations is beneficial for both operators and users. As EV charging stations are commercial emergency service facilities, the CS location should be determined to maximize user satisfaction while considering various costs for the operator, aiming to increase the profitability of the charging station. The proposed model in this paper comprehensively considers user capture, travel cost from demand nodes to charging stations, and the total construction cost of the charging station.

#### (1) User Capture Degree $C_1$

To increase the utilization and operational efficiency of CSs, it is essential to consider the potential amount of EV users within the service range when constructing CSs. Let  $w_i$  represent the weight of road nodes, where a larger weight implies more potential EV users near the node. Assuming the shortest distances from user trip origins and destinations, as well as charging demand points to the charging station, are determined using the Dijkstra shortest path algorithm. To serve more EV users, the objective function maximizes the user capture degree, given by:

$$\max C_1 = \sum_{n \in N} x_n (f_{n1} + f_{n2}) \quad (22)$$

$$f_{n1} = \sum_{m \in M} w_m w_n x_m x_n L_{mn} \quad (23)$$

$$f_{n2} = \sum_{m \in M} w_m w_n x_m (1 - x_n) L_{mn} \quad (24)$$

where  $f_{n1}$  and  $f_{n2}$  represent the user capture degree when constructing and not constructing a charging station at node  $n$ , respectively.  $w_m$  and  $w_n$  denote the weights of EV trip origins and charging station  $n$ , respectively.  $x_m$  and  $x_n$  are 0–1 decision variables indicating whether a charging station is constructed at EV demand point  $m$  and node  $n$ , respectively.

#### (2) Travel Energy Cost for Charging $C_2$

The total travel cost of EV mainly refers to the energy consumption cost from the demand point to the charging station, given by:

$$\min C_2 = \sum_{m=1}^M \sum_{n=1}^N \eta_{mn} x_n C_{mn}^{\text{char}} \quad (25)$$

$$C_{mn}^{\text{char}} = \kappa \times T_{mn}^{\text{char}} \quad (26)$$

where  $\eta_{mn}$  is the number of EVs traveling from demand point  $m$  to charging station  $n$ .  $C_{mn}^{\text{char}}$  stands for the charging cost for EV from demand point  $m$  to charging to the battery's rated capacity at charging station  $n$ .  $\kappa$  is the charging price per unit time, related to the charging time period.  $T_{mn}^{\text{char}}$  represents the estimated charging time for EV from demand point  $m$  to charging to the initial charge state at charging station  $n$ .

The existing fast-charging stations typically employ a two-stage charging strategy with a fast-charging machine. Initially, the fast-charging machine can continuously charge at a high power for about half an hour until the battery reaches approximately 80 % of its rated capacity. Afterward, it switches to a lower power level for slow charging, aiming to protect the battery. Therefore, the EV charging time refers to the estimated duration it takes for the vehicle to charge from the current remaining battery level to a state of charge of 80 % after arriving at charging station  $n$ . Hence, the quantity of electricity,  $E_{mn}^{\text{char}}$ , and the charging time for EV charging from demand point  $m$  to charging station  $n$ ,  $T_n^{\text{char}}$ , are given by:

$$E_{mn}^{\text{char}} = 80\% E_{\max} - E_{\max} s_m - E_{mn} \quad (27)$$

$$T_{mn}^{\text{char}} = \frac{E_{mn}^{\text{char}}}{P_{\text{char}}} \quad (28)$$

where  $E_{\max}$  is the rated capacity of the EV battery.  $s_m$  denotes the remaining state of charge when EV departs from demand point  $m$ .  $P_{\text{char}}$  represents the rated power output of the charging pile.

#### (3) Charging Station Construction Cost $C_3$

To meet the demands of urban EV users and ensure the operator's interests, there is a tendency to set up as many charging and swapping stations as possible when constructing shared EV energy supplement stations. However, the construction of EV charging stations requires a significant amount of urban land resources, involving costs such as land leasing, construction, and operation management. Additionally, the large number of EV charging stations has a considerable impact on the regional power quality. Therefore, it is necessary to consider various costs of charging stations and determine an appropriate number of CS constructions. The construction cost for setting up a charging station at node  $n$  is given by:

$$\min C_3 = \sum_{n=1}^N (C_n^{\text{rent}} + C_n^{\text{build}} + C_n^{\text{oper}}) x_n \quad (29)$$

where  $C_n^{\text{rent}}$ ,  $C_n^{\text{build}}$ , and  $C_n^{\text{oper}}$  represent the costs for land leasing, construction, and operation management, respectively, when constructing a charging station at node  $n$ .

Based on the aforementioned considerations, this paper uses the entropy weight method to construct the total social cost indicator  $F$  as the optimization objective, formulated as Equation (30).

$$\min F = -\lambda_1 C_1 + \lambda_2 C_2 + \lambda_3 C_3 \quad (30)$$

s.t.

$$\sum_{n \in N} x_n \leq N_s \quad (31)$$

$$T_{mn} \leq T_{\max}, \forall m \in M, n \in N, t \in T \quad (32)$$

$$\sum_{n \in N} d_n x_n \leq P_n, \forall n \in N \quad (33)$$

$$L_{mn} \leq L_{\max}, \forall m \in M, n \in N \quad (34)$$

$$s_m \leq E_{\max}, \forall m \in M, n \in N, t \in T \quad (35)$$

$$x_n, y_{ij} \in \{0, 1\}, \forall n \in N, \forall i, j \in V \quad (36)$$

where  $F$  represents the total social cost of the charging station location scheme.  $x_n$  is a 0-1 decision variable representing where to construct a charging station at node  $n$ .  $N_s$  denotes the maximum number of planned EV charging stations in the region.  $T_{\max}$  is the isochrone parameter of the CS service range.  $d_n$  stands for the charging demand within the service range of charging station  $n$ .  $P_n$  denotes the number of charging piles at charging station  $n$ .  $L_{\max}$  represents the maximum distance that an EV user can accept when choosing a charging station, which is generally related to the remaining charge level of the EV and can be set as the range that can be driven by 20 % of the EV battery capacity.  $\lambda_1$ ,  $\lambda_2$ , and  $\lambda_3$  are the weight coefficients for user capture degree, travel cost, and construction cost, respectively. These coefficients can be determined using the entropy weight method, which is given by Equation (37) through (39).

The model constraints are shown in Equation (31) through (36). Equation (31) represents the constraint on the quantity of proposed charging stations. Equation (32) constrains the travel time service range of the proposed charging stations. Equation (33) indicates the capacity constraint of the charging station. Equation (34) restricts the maximum distance an EV user can accept when selecting a charging station. Equation (35) represents the energy consumption constraint for EVs traveling to the charging station. Equation (36) depicts the binary decision variable constraint.

The values of  $\lambda_j$  ( $1 \leq j \leq 3$ ) have an important impact on the final selection of the location selection scheme. In this paper, the entropy weight method is used to determine their values. The entropy weight method is an objective weighting method that utilizes the information provided by the entropy value of each indicator to determine the weight of the indicators. It can avoid interference from subjective factors, making the evaluation results more in line with reality. The information entropy of the  $j$ -th evaluation indicator (i.e., cost  $C_j$ ) is:

$$E_j = -\eta \sum_{i=1}^Y p_{ij} \ln p_{ij}, 1 \leq j \leq 3 \quad (37)$$

where  $Y$  represents the number of candidate schemes.  $\eta$  is a coefficient, which equals  $1/\ln n^*$  and  $n^*$  is the number of evaluation indicators and  $n^* = 3$  here.  $p_{ij}$  denotes the proportion of the  $j$ -th evaluation indicator under the  $i$ -th candidate scheme, calculated as follows:

$$p_{ij} = -\frac{r_{ij}}{\sum_{i=1}^Y r_{ij}} \quad (38)$$

where  $r_{ij}$  is the value of  $j$ -th evaluation indicator under the  $i$ -th candidate scheme.

The weight of  $j$ -th evaluation indicator,  $\lambda_j$ , is computed as:

$$\lambda_j = \frac{(1 - E_j)}{\sum_{j=1}^3 (1 - E_j)} \quad (39)$$

#### 4. Adaptive Co-evolutionary clustering algorithm

The CEOLRP (co-evolutionary optimization model of location-routing problem) consists of two sub-problems: facility location and the shortest path problems. Some Location-Routing Problem (LRP) algorithms adopt a cluster-firs route-second strategy, treating the LRP problem as separate components. However, facility location and the shortest path problems are mutually influential, where the facility

location results impact the shortest route, and the shortest route between demand points and CSs reciprocally affects the CS location scheme [51]. Therefore, this paper integrates the coevolutionary mechanism of the Improved Ripple Spreading Algorithm (IRSA) and the clustering framework of the K-means algorithm, designing a two-stage ACECA (adaptive co-evolutionary clustering algorithm). This algorithm can effectively simulate the spatiotemporal variation characteristics of demand points and the traffic environment, collaboratively solving the two sub-problems of CEOLRP, thereby enhancing the ability to search for optimal solutions.

##### 4.1. Adaptive clustering framework of ACECA

Existing clustering algorithms not only require specifying the number of clusters in advance but also are sensitive to data noise and outliers, making it challenging to handle data with time-varying features. To address these issues, this paper develops an adaptive search strategy for determining the optimal number of clusters based on a clustering framework, and adopts a global traversal approach to parallelly search the peripheral region of initial clusters (whose range is determined by the search radius  $R$ ) in order to determine the optimal spatial positions of each cluster. Simultaneously, to handle the time-varying features of the data, the ACECA incorporates the parameters related to the shortest path between demand points and clusters in time-varying traffic environments as clustering weights during the clustering process, thus transforming the uncertain data into deterministic weights. The principle of the adaptive clustering framework of the ACECA is illustrated in Fig. 2.

**Step 1.** Data Initialization. Set the value range for the number of clustering centers  $N_n$ ,  $N_n \in [N_{\min}, N_{\max}]$ . Let  $k = 0$ .

**Step 2.** Network Generation. Set  $N_n = N_{\min} + k$ . Construct an extended space-time-state network based on the spatiotemporal distribution of charging demand. Generate  $N_m$  EV charging demand points and  $N_n$  initial positions of clustering centers, denoted as  $K_i$  ( $i = 1, 2, \dots, n$ ).

**Step 3.** Cluster Assignment. Utilize the co-evolutionary mechanism of the IRSA to dynamically optimize the path with minimum travel time,  $P_{mn}$ , from each demand point to the clustering center in the space-time-state network (see Section 4.2). Assign demand points to the cluster corresponding to  $K_i$ , the clustering center with the minimum travel energy consumption.

**Step 4.** Expand the solution space of each cluster and update the cluster center. Calculate the average value from the demand point to the cluster center in each cluster as the candidate cluster center  $K_i^*$ , and then label all nodes within a  $R$  radius around  $K_i^*$  as neighboring candidate cluster centers, as shown in Fig. 3. Traverse each candidate cluster center and calculate the total social cost  $F$  from all demand points of the corresponding cluster to the candidate cluster center  $K_i^*$ . Finally, select the candidate cluster center with the lowest  $F$ -value as the new cluster center for the next iteration.

**Step 5.** Iteration and Termination of Clustering Process. Reclassify demand points to the clusters based on the new clustering centers, then return to Step 3 until the clustering centers no longer change. By continuously updating the positions of clustering centers, the social total cost of CS location is reduced iteratively. When the clustering centers remain unchanged or the spatial distance between cluster centers in adjacent iterations,  $D(k-1, k)$ , meets the convergence condition  $D(k-1, k) \leq CT$ ,  $K_i^*$  is considered the final location for EVCS.

**Step 6.** Global Traversal for Optimal Number of Clusters. If  $n < N_{\max}$ , set  $k = k + 1$  and return to Step 2; otherwise, the number and location of clustering centers with smallest  $F$ -value is defined as the final CS location scheme.

Suppose the number of EV charging demand points is  $N_m$ , the data

---

Algorithm 1: Algorithm framework for collaborative operation of adaptive clustering and path optimization processes

---

```

1: initialize  $N_{\min}$ ,  $N_{\max}$ ,  $m$ ,  $R$ ,  $CT$ 
2: initialize  $N_n = N_{\min}$ 
3: while  $N_n \leq N_{\max}$  do
4:   generate expanded network
5:   generate  $N_m$  charging demand points
6:   generate  $N_n$  cluster centers  $K = [K_1, K_2, \dots, K_n]$ 
7:   iteration = 0
8:   repeat
9:     use the IRSA algorithm to find the optimal path  $P_{mn}$ 
10:    assign points to clusters
11:    for  $i = 1$  to  $N_n$  do
12:      compute average clustering centers  $K_i^*$ 
13:      mark the neighboring centers of  $K_i^*$  according to  $R$ 
14:      compute social total cost of neighboring centers
15:      find the center point  $K_i^*_{\text{min}}$  with the lowest social total cost
16:      if  $D(K_i^*_{\text{min}}, K) \leq CT$  then
17:        break // Terminate the iteration if the cluster centers no longer change
18:      end if
19:       $K = K_i^*_{\text{min}}$ 
20:      iteration = iteration + 1
21:    until false
22:     $N_n = N_n + 1$ 
23: end while
24: Finding the number of cluster centers with the lowest total social cost as the final scheme
25: return final cluster centers

```

---

**Fig. 2.** Adaptive clustering framework of ACECA.

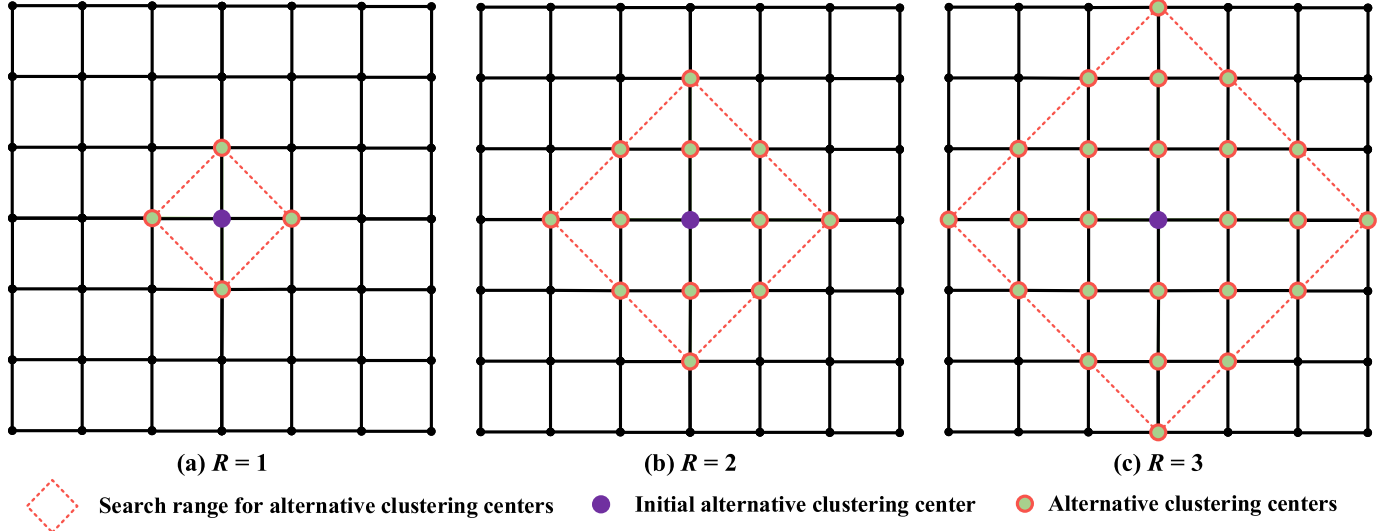


**Fig. 3.** Candidate cluster centers within search ranges of different radius values  $R$ .

dimension is  $N_d$  and the number of iterations to complete a clustering optimization process is  $N_{\text{iter}}$ . The number of clusters required to obtain the final result is  $N_{\max} - N_{\min} + 1$ . Then, the computational time complexity of the adaptive clustering framework for realizing ACECA can be assessed as  $O(N_{\text{iter}} \times N_m \times (N_{\max} - N_{\min} + 1) \times N_d)$ .  $N_m$ ,  $N_d$ ,  $N_{\text{iter}}$ ,  $N_{\max} - N_{\min} + 1$  are generally considered constants. Similar to K-means, the computational complexity of adaptive clustering framework for realizing ACECA is linear.

#### 4.2. Co-evolutionary optimization mechanism of ACECA in dynamic traffic environment

This study designs an Improved Ripple Spreading Algorithm (IRSA) for path optimization and coordinated evolution of traffic environment, which outputs the shortest path with the minimum travel time. The basic

idea of the IRSA algorithm is to continuously run the ripple relay process guided by time units, so that the ripple spreads from the starting point and traverses other nodes until it reaches the endpoint for the first time, and finally outputs the optimal path [52]. The ripple relay is illustrated in Fig. 4, in which the node states can be classified into four types, i.e., inactivated, waiting, activated, and dead, to reveal the evolution of the traffic over time, due to the co-evolution of the ripple diffusion process with the traffic environment in road network [53]. When the ripple reaches an inactive node, it activates the node and generates new ripples to propagate to surrounding inactive nodes, and so on. It's worth noting that new ripples no longer propagate to the activated nodes, reducing redundant computations. When the ripple reaches a blocked node, the ripple state of the node will be transformed into a waiting state until the blocked state of the node is transformed into accessible, which simulates the scenario of EV stopping and waiting when encountering a red signal

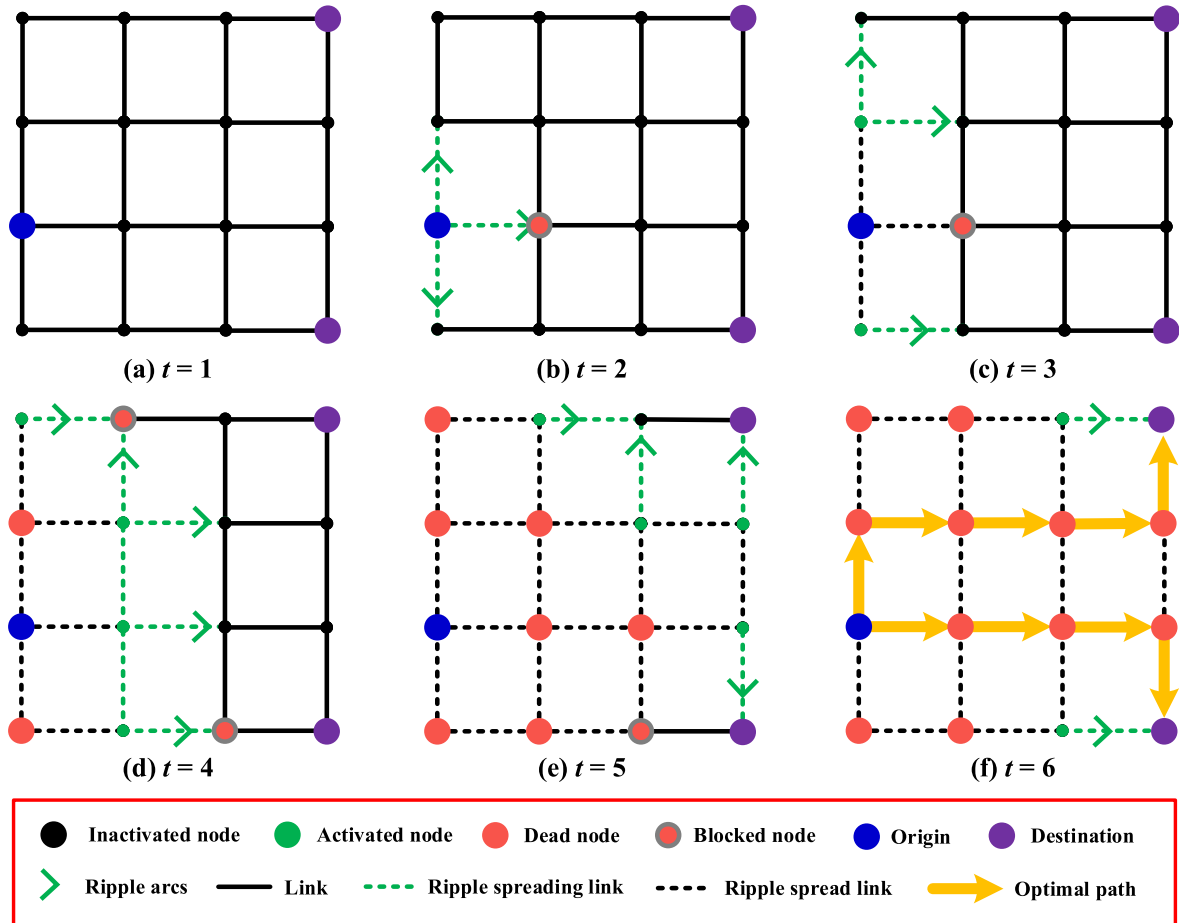


**Fig. 4.** Illustration of ripple relay co-evolving with time-varying traffic environment.

at a signalized intersection. During the ripple relay process, all ripples compete with different propagation speeds consistent with the average driving speeds of EVs, changing as the road network traffic environment evolves. Except for the starting point, when all the nodes around a particular node have been activated by ripples, the node enters a dead state. The ripple relay stops when ripples from a starting point traverse all endpoints. Subsequently, the source of the ripples that activated each endpoint is traced back to obtain the information of the previous node, and so on, and the backtracking process is looped until a complete optimal path is formed between the starting point and all the endpoints.

To simplify the problem description without loss of generality, this study assumes there are  $N_N$  nodes in the road network, with demand point  $m$  as the starting point and charging station  $n$  as the endpoint. In the ripple relay, node  $i$  can only be triggered once, and the ripple generated is referred to as ripple  $i$ , which can split into a maximum of four segments. Each segment's propagation speed and direction vary, revealing the connectivity between node  $i$  and its adjacent nodes, reflecting the spatiotemporal diversity of traffic flow states in the urban road network. Let  $S_R(i)$  represent the state of ripple  $i$ , where  $S_R(i) = 0, 1, 2, 3$  indicates the states of ripple  $i$  are inactive, waiting, active, and dead, respectively.  $R^*(i)$  denotes the set of propagation radii for each segment of ripple  $i$ .  $r(i,j)$  represents the propagation radius from node  $i$  to node  $j$ , and  $r(i,j) \in R^*(i), i \neq j$ .  $V_{t+k}^*(i)$  stands for the set of propagation speeds for each segment of ripple  $i$ , and  $\bar{v}_{t+k}(i,j) \in V_{t+k}^*(i), i \neq j$ . Here,  $V_{t+k}^*(i)$  and  $R^*(i)$  are mutually corresponding, representing different dimensions of the same ripple.  $F_R(i)$  is the variable recording the source node of the ripple that activates node  $i$ , where  $F_R(i) = j$  indicates that node  $i$  was activated by the ripple of node  $j$ , and  $F_R(i) = 0$  represents that node  $i$  is in an inactivated state. When the endpoint is activated by a ripple, the

optimal path  $P_{mn}$  can be derived from  $F_R(n)$  using iterative backtracking method, formulated as follows:

$$P_{mn}(i) = \begin{cases} n, i = L(P_{mn}) \\ F_R[P_{mn}(i+1)], i < L(P_{mn}) \end{cases} \quad (40)$$

where  $L(P_{mn})$  represents the number of nodes in path  $P_{mn}$ , and  $P_{mn}(i)$  denotes the  $i$ -th node in path  $P_{mn}$ .

To objectively reflect the time-varying characteristics of traffic flow on each road segment, the order in which the ripple visits nodes is recorded. The length of ripple diffusion in each time unit must be less than the length of the shortest road segment to avoid the possibility of losing ripple visit records. Therefore, it is necessary to choose an appropriate time unit  $t_u$  to describe the periodicity of changes in traffic environments in road segments and ensure the completeness of ripple visit records. The time unit  $t_u$  is subject to the following constraint:

$$0 \leq \bar{v}_{t+k}(i,j) \times t_u \leq L_{min} \quad (41)$$

where  $L_{min}$  denotes the shortest length among all road segments in the road network, and  $t_u$  represents the time unit.

The main steps of the IRSA based on the co-evolutionary mechanism in a time-varying network are illustrated in Fig. 5.

Suppose each node has  $N_{AC}$  links on average, and it takes  $N_{ATU}$  time units on average for a ripple to travel through a link. Then, the computational complexity of the IRSA for solving an optimal path  $P_{mn}$  can be assessed as  $O(N_N \times N_{AC} \times N_{ATU})$  [52]. Considering that  $N_m$  paths between CSs and EVs need to be calculated for each clustering iteration, thus, the computational complexity of ACECA is  $O(N_N \times N_{AC} \times N_{ATU} \times N_{iter} \times N_m^2 \times (N_{max} - N_{min} + 1) \times N_d)$ .

---

Algorithm 2: IRS algorithm based on coevolutionary mechanism in *Space-Time-State Network* networks

---

```

1: for  $i = 1$  to  $N_N$  do
2:    $F_R(i) = 0$ ,  $R^*(i) = 0$ ,  $S_R(i) = 0$ 
3:   let  $k = 0$ ,  $S_R(m) = 2$ ,  $t = 0$ 
4:   if  $F_R(n) > 0$  then
5:     trace back the ripple activation sequence and output the optimal path  $P_{mn}$ 
6:   else if  $F_R(n) = 0$  then
7:     for  $i = 1$  to  $N_N$  do
8:       if  $S_R(i) = 1$  and  $F_R(i) > 0$  then
9:          $S_R(i) = 2$ 
10:        end if
11:        if  $i$  is accessible and  $S_R(i) = 2$  then
12:          let  $r(i, j) = r(i, j) + \bar{v}_{t+k}(i, j) \times t_u$ 
13:        end if
14:      end for
15:      for  $i = 1$  to  $N_N$  do
16:        if  $i$  is accessible and activated by at least one ripple then
17:          assume that the ripple of  $q$  is the first to reach  $i$ ,  $j$  is the neighboring node of node  $i$ , let
18:             $r(i, j) = r(q, i) - l_{qj}$ ,  $F_R(i) = q$ ,  $S_R(i) = 2$ 
19:        end if
20:        if  $i$  is blocked and activated by at least one ripple then
21:          assume that the ripple of  $q$  is the first to reach  $i$ , let  $F_R(i) = q$ ,  $R^*(i) = 0$ ,  $S_R(i) = 1$ 
22:        end if
23:        if  $F_R(q) > 0$  for every  $q$  that is adjacent to node  $i$  then
24:           $S_R(i) = 3$ 
25:        end if
26:      end for
27:    end if

```

---

**Fig. 5.** Main steps of the IRS.

## 5. Experimental analysis

To validate the effectiveness of the CEOLRP model and ACECA algorithm, three sets of simulation experiments were designed based on two types of transportation networks (deterministic and uncertain). The first set is a parameter optimization experiment, examining the influence of the search radius  $R$  and the number of clustering centers  $N_c$  on the performance of the ACECA algorithm in different transportation networks. The second set of experiments were designed to compare the performance of ACECA, genetic algorithm (GA), immune algorithm (IA), particle swarm optimization (PSO), grey wolf optimization (GWO) and K-means clustering algorithm in CS location optimization under deterministic and uncertain transportation networks, respectively. Among them, the weights between demand points and CS in the GA, IA, PSO, GWO and K-means algorithms are obtained based on the Dijkstra algorithm to derive the shortest path. The third set of experiments analyzed the impact of road network scale, traffic volume, and charging station capacity on the model results, which aim to explore the potential application of the proposed model.

While the evolution of the traffic environment on the road network can be predicted, achieving 100 % accuracy in prediction data is difficult. Therefore, when constructing scenarios for an uncertain transportation network, the average traveling speed of road segments across the entire network changes over time, and its value may deviate from actual data, reflecting the uncertainty characteristics of the extended space-time-state network in Section 3.3. Due to the general limitations of current intelligent algorithms, errors in predicting traffic flow parameters tend to increase over time. The predicted value of the average travel speed of road segment  $(i, j)$  at time unit  $t + k$  is given by:

$$\bar{v}_{t+k}(i, j) = \bar{v}_{t+k}^*(i, j) \pm \epsilon_{t+k}(i, j) \quad (42)$$

$$\epsilon_{t+k}(i, j) = \phi \times k + \tau \times \bar{v}_{t+k}^*(i, j) \quad (43)$$

where  $\bar{v}_{t+k}(i, j)$  and  $\bar{v}_{t+k}^*(i, j)$  represent the predicted value and actual

value of the average travel speed of road segment  $(i, j)$  at time  $t + k$ , respectively.  $\epsilon_{t+k}(i, j)$  denotes the prediction error of the average travel speed of section  $(i, j)$  at time  $t + k$ .  $\tau$  stands for the initial prediction error rate of the average travel speed.  $\phi$  is the rate at which the prediction error of the average travel speed accumulates over time.

In this section, we conduct all experiments related to uncertain transportation network scenarios with  $\tau = 0.1$ ,  $\phi = 0.1$ . Instances are generated based on a squared virtual road network. Each node can connect to at most four other nodes. The distance between any two nodes is randomly distributed between 200 m and 400 m. The number of EV charging demand points  $N_m$  is 45, with the daily charging demand for each point randomly distributed between 1 and 10. The average travel speed in road segments is randomly set between 30 km/h and 60 km/h, and the average travel delay of nodes is randomly distributed between 30s and 90s.

### 5.1. Experiment 1: algorithm parameter optimization

The principle objective of the location optimization algorithms is to achieve global optimality, which is a crucial indicator for evaluating algorithm performance. The search radius  $R$  and the number of clustering centers  $N_c$  are two key parameters affecting the optimization performance of the ACECA algorithm.

#### 5.1.1. Influence of search radius $R$ on ACECA performance

The algorithm's ability to find the optimal solution is strengthened with a larger search radius  $R$ , as it traverses a larger solution space globally. However, this also increases computation time. To enhance performance, it is necessary to choose the optimal search range during the clustering iteration process. Fig. 6 shows the relationship between numerical changes in  $R$  and optimization results of the algorithm across different road network scales ( $N_N = 100$  and 400).

From Fig. 6, it can be observed that in the deterministic transportation network scenario, construction cost, travel energy cost, and total social cost all decrease slightly with the increasing  $R$ , while the

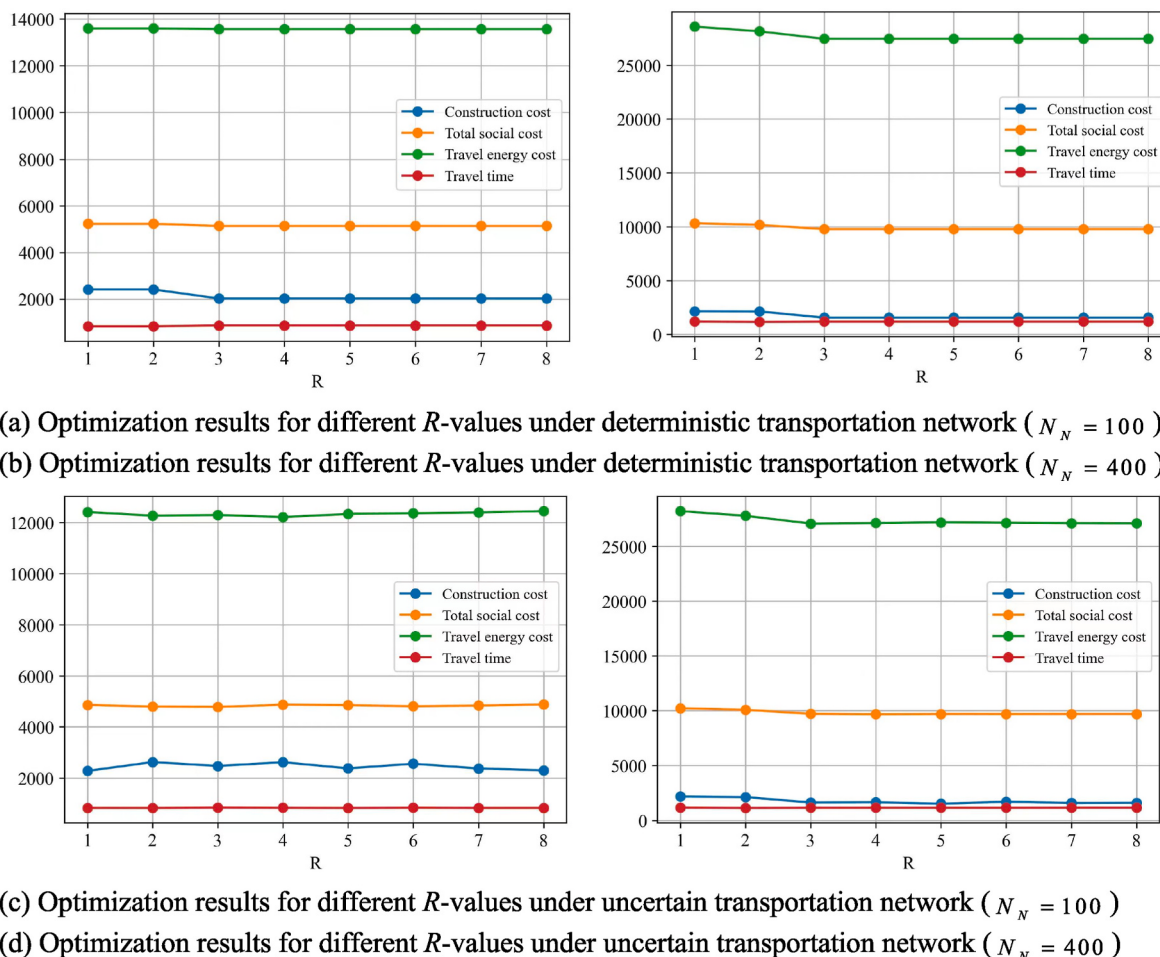


**Fig. 6.** The effect of different search radii  $R$  on the location results.

travel time of EVs remains fundamentally unchanged. Among them, these trends are more significant in the road network with 400 nodes ( $N_N = 400$ ). When the value of  $R$  is no less than 3, all kinds of costs remain unchanged, which indicates that the positive effect of expanding the search radius on the algorithm's optimization capability has reached saturation.

In the uncertain transportation network scenario, under the road network containing 100 nodes ( $N_N = 100$ ), both the construction cost and the trip energy consumption cost show a tendency of slight oscillatory fluctuation as  $R$  increases, while the trip time and the total social cost remain basically unchanged. This may be due to the fact that the uncertainty of the transportation environment significantly interferes with the iterative process of the algorithm, weakening the positive benefits of  $R$  in enhancing algorithm capability to some extent. Under the road network containing 400 nodes, the construction cost, trip energy consumption cost, and total social cost decrease slightly as  $R$  increases, while the EV travel time remains basically unchanged. Similar to the deterministic scenario, when  $R$  is no less than 3, all types of costs remain constant. This indicates that although the uncertainty of the traffic environment inhibits the positive effects of expanding  $R$ , the optimization capability of ACECA remains stable, demonstrating strong robustness. Therefore, to obtain better algorithm optimization capability, the  $R$ -value is set to 3 for all subsequent experiments.

#### 5.1.2. Impact of the number of clustering centers on ACECA performance

The number of clustering centers  $N_c$  is a prerequisite for the clustering algorithm to start optimization, and its value is closely related to the economic and environmental benefits of the CS location scheme. To

highlight the significant improvement of ACECA with an adaptive clustering strategy in optimizing performance compared to traditional clustering algorithms, the influence of different numbers of clustering centers on location plans in different road network scales are shown in Fig. 7.

Fig. 7 shows that the sensitivity analysis results of  $N_c$  obtained by ACECA in both deterministic and uncertain transportation networks are generally consistent. As  $N_c$  increases, both the total social cost and construction cost initially decrease and then increase. Meanwhile, the energy consumption and travel time of EVs generally decrease. When  $N_c$  is greater than or equal to 4, both the total social cost and construction cost decrease as  $N_c$  increases. This is primarily due to the significant impact of construction cost on the total social cost, and the ACECA's preference for a location scheme with a smaller total construction cost during the optimization process, with the aim of minimizing the overall social cost. In summary, the construction cost of a location scheme with more charging stations is not necessarily higher than that of a scheme with fewer charging stations. Additionally, the cost is also influenced by the spatial layout of the charging stations.

Moreover, the increase in the number of charging stations significantly reduces the energy consumption cost of EVs, further lowering the overall social cost. When  $N_c$  is no less than 4, the increasing construction costs of each charging station contribute to the rising total construction cost of the location scheme. This indicates that the cost inflation brought about by the increasing number of charging stations surpasses the benefits of optimizing the spatial layout of charging stations. Since EVs tend to charge at nearby stations, a higher number of charging stations usually results in lower travel energy consumption and travel time,

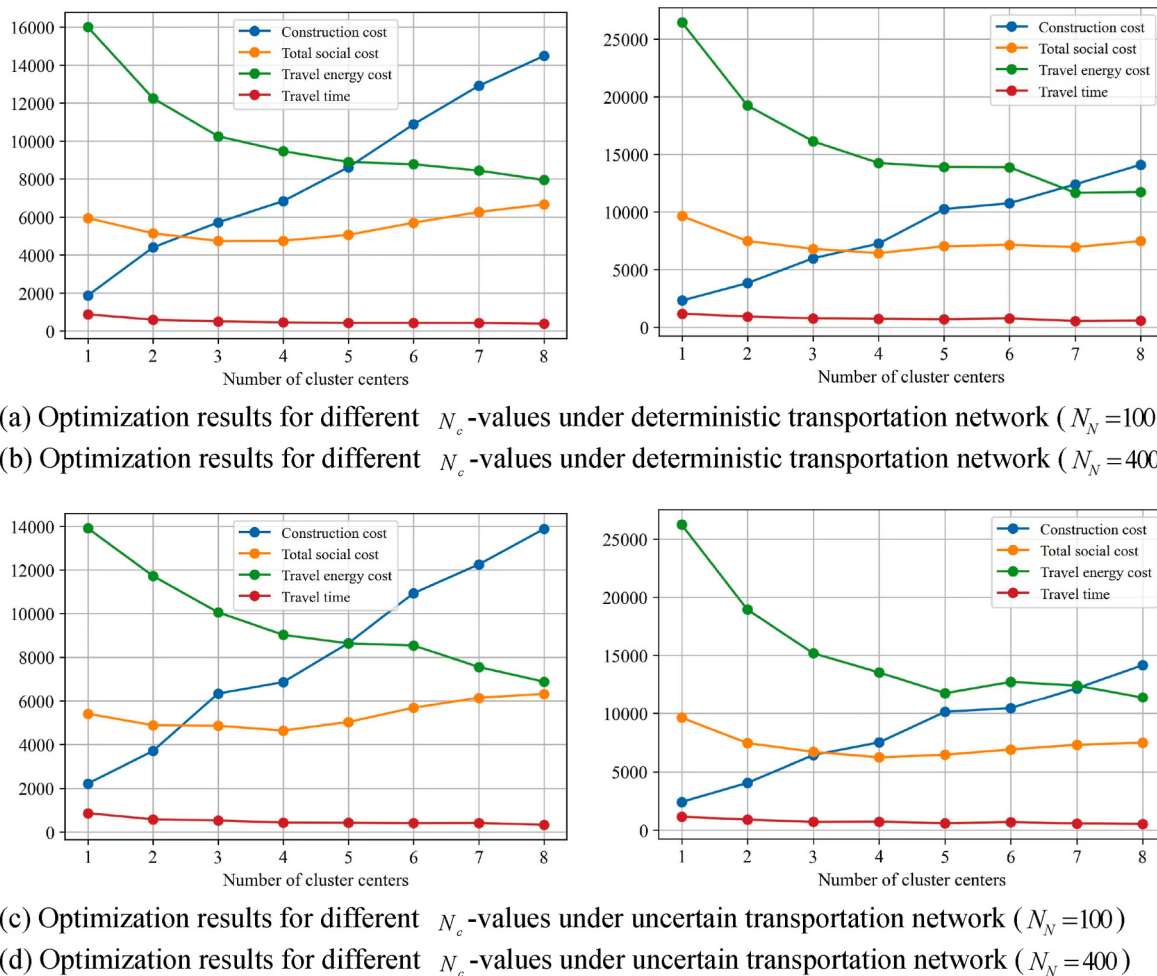


**Fig. 7.** The effect of different numbers of clusters  $N_c$  on the location results.

leading to increased convenience for users and a reduction in traffic carbon emissions. Therefore, the ACECA algorithm, with its adaptive clustering strategy, can enhance the economic and environmental benefits of the location scheme by optimizing the number of charging stations.

## 5.2. Experiment 2: robustness analysis

In order to compare the proposed ACECA to K-means, GA, IA, PSO and GWO algorithms, we conduct the simulation experiment in deterministic ( $\tau = 0, \phi = 0$ ) and uncertain ( $\tau = 0.1, \phi = 0.1$ ) networks. Taking the network with 400 nodes as an example, the results are pre-

sented in **Table 1**.

As can be seen from **Table 1**, the CS location selection scheme obtained by ACECA is superior to the other five algorithms in terms of total social cost, average travel time, total travel distance and travel energy cost. In terms of total social cost, ACECA yields the best location results, followed by K-means, with GWO being the least effective. Specifically, the total social cost of the ACECA result is at least 20.30 % and 18.85 % lower than that of results obtained by other methods for deterministic and uncertain networks, respectively. This is mainly because ACECA not only considers the spatiotemporal heterogeneity of charging demand in dynamic traffic environments to optimize the spatial layout of CS, but also optimizes the number of CS through adaptive clustering strategy,

**Table 1**

Optimization results by different algorithms in deterministic and uncertain networks ( $N_N = 400$ ).

	Algorithms	Total Social Cost	Travel Energy Cost (yuan/day)	Construction cost (yuan/day)	Average Travel Time (min)	Total Travel Distance (km)	Computation Time (min)
$\tau = 0, \phi = 0$	ACECA	<b>6664.36</b>	<b>13777.45</b>	<b>8939.00</b>	<b>9.88</b>	<b>1194.00</b>	<b>9.62</b>
	K-means	8017.20	19213.98	6656.31	15.61	1624.24	4.64
	GA	8423.50	20728.30	6021.88	18.82	1856.28	60.07
	IA	10876.97	26878.70	7569.80	25.29	2499.63	59.35
	PSO	8891.07	21612.27	6839.35	21.29	1933.73	31.07
$\tau = 0.1, \phi = 0.1$	ACECA	<b>6688.86</b>	<b>14169.54</b>	<b>8473.76</b>	<b>9.80</b>	<b>1237.22</b>	<b>9.02</b>
	K-means	7949.87	19193.89	6449.61	14.34	1543.68	22.71
	GA	8734.00	21136.76	6886.93	21.58	2003.17	65.28
	IA	9191.75	22274.38	7194.35	18.78	1987.07	57.50
	PSO	8758.59	21321.11	6681.75	18.69	1918.33	32.91
	GWO	9803.07	24175.72	6912.20	23.28	2229.85	61.05

further reducing the total social cost.

In terms of average travel time and total travel distance, ACECA obtains the best results, followed by K-means, and GA, IA, PSO yield similar results. Since the results obtained by six algorithms can be ranked in the similar order in terms of travel time and travel distance, we take the average travel time as an example to discuss in detail. The average travel times of ACECA results in deterministic and uncertain networks are 9.88 min and 9.80 min, respectively, which are shorter than that of results by other algorithms by at least 57.96 % and 46.36 %, respectively. This is mainly because ACECA selects candidate cluster centers initially based on the shortest path from each demand point to cluster centers obtained by IRSAs. Therefore, ACECA guarantees shorter travel times while minimizing the total social cost of the site selection scheme.

With respect to travel energy costs, ACECA obtains the best results, followed by K-means, with IA and GWO being the least effective in deterministic and uncertain networks, respectively. The daily average travel energy costs of ACECA results in deterministic and uncertain networks are lower than that of results by other algorithms by at least 39.46 % and 35.46 %, respectively. This is mainly because ACECA utilizes IRSAs to obtain paths with smaller travel times and distances in the cluster assignment process, meaning that the travel energy consumption between demand points and clustering centers is smaller than other algorithms. Additionally, ACECA, guided by minimizing travel energy costs, allocates demand points to the clusters corresponding to the clustering centers, further reducing the travel energy consumption of CS locations. Finally, the adaptive optimization of the number of cluster centers by ACECA may indirectly reduce travel energy costs.

Regarding construction costs, the results solved by ACECA are not advantageous compared to other algorithms, especially in deterministic network. This is mainly due to the fact that ACECA may reduce the total social cost and trip energy cost by adding more clustering centers, but the increase in the number of clustering centers usually increases the construction cost. In terms of computational efficiency, ACECA and K-means have significant advantages, with shorter computation time compared to other algorithms.

In summary, although ACECA's performance in reducing construction costs of CS location schemes is suboptimal, it excels in reducing total social costs, decreasing travel times, and promoting energy conservation and emission reduction. It is worth noting that, after introducing uncertainty disturbances, ACECA's numerical changes in key evaluation indicators such as total social cost, travel time, and travel distance do not exceed 4 %. Compared with other algorithms, ACECA demonstrates excellent robustness in uncertain transportation networks. Since the CS location needs to consider multiple factors such as economy, efficiency, uncertainties, environmental protection, and user convenience, ACECA is more suitable for solving the multi-objective CS location problems.

### 5.3. Experiment 3: sensitivity analysis

To explore the potential application of the proposed model, the sensitivity analysis experiments are conducted to analyze the impact of road network size, traffic volume, and charging station capacity on the model results.

#### 5.3.1. Network size

The scale of the road network is an important factor affecting the efficiency and portability of the algorithm. To explore the potential application of the proposed method in cities with different network scales, we conducted simulation tests on road networks with scales of  $N_N = 100, 225, 400, 625, 900$ . The computation time is shown in Fig. 8. The computation time of ACECA increases with the increase in the scale of the road network. When the scale of the road network is less than 625, the computation time for ACECA to solve the CS location selection scheme is generally controlled within 12 min. When the scale of the road

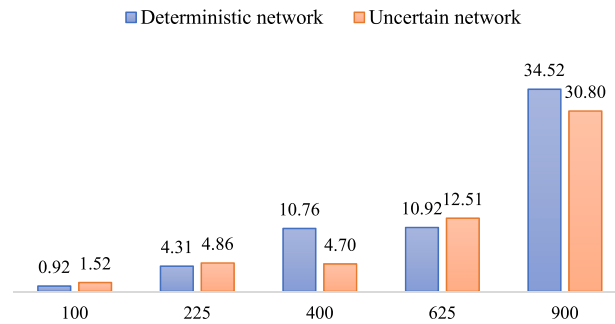


**Fig. 8.** Computation time of ACECA for different road network scales (in minutes).

network increases to 900, the computation time of ACECA significantly increases for both deterministic and uncertain networks, reaching 34.52 min and 30.80 min, respectively. This is mainly because ACECA requires a considerable amount of computation for calculating the shortest paths between sites and demand points during the location selection process. However, the complexity of solving the shortest paths is significantly influenced by the scale of the road network, which adds to the iterative calculation process of ACECA, leading to a rapid increase in computation time. Fortunately, the location selection problem for charging stations does not require high timeliness in model solving but values the quality of location selection solutions, making it more tolerant of algorithm computation time. Although ACECA has relatively large computation time on large-scale road networks, this does not mean it is unsuitable for practical applications. In fact, Experiment 2 has already demonstrated the superiority of ACECA in terms of efficiency in solving.

#### 5.3.2. Traffic volume

Traffic volume is closely related to the average travel speed of road segments [54,55]. Generally, the higher the traffic volume means the lower average travel speed of road segments. To analyze the impact of traffic volume on the model results, we simulated the traffic operating conditions under different traffic volumes by adjusting the fluctuation range of the average travel speed of road segments. The fluctuation ranges of the average travel speed of road segments are [10, 30), [30, 50), and [50, 70], with units in km/h, representing high, medium, and low traffic volume, respectively. Taking  $N_N = 400$  as an example, the results are shown in Table 2 and Fig. 9.

Table 2 and Fig. 9 display that the CS location selection solutions vary with different levels of traffic volume. For CS's location selection solutions with higher traffic volumes, the total social cost, travel energy cost, and construction cost are lower, however, travel time and distance raise. It's noteworthy that as the traffic volume decreases, the travel distance, travel time, and computation time for ACECA to solve location selection solutions become shorter. This may be because when there are more congested segments in the road network, the average travel speed of each segment tends to be lower, and ACECA avoids congested segments, resulting in increased detour distance and travel time. Furthermore, since the evolution of future traffic conditions is time-oriented, the computation time is positively correlated with travel time. That is, the greater the travel time, the longer the computation time. Therefore, applying the method proposed in this paper to design EVCS location selection solutions in cities with high daily traffic volumes can reduce the construction costs of operators and travel energy consumption of EV users, leading to higher economic and environmental benefits. On the other hand, applying this method in cities with lower traffic volumes can effectively reduce the time and distance required for users to travel to charging stations, thereby enhancing the user charging experience. However, the increase in the number of charging stations will also increase the economic investment of operators.

**Table 2**

Results under different levels of traffic volume.

Traffic Volume	Speed Range (km/h)	Total Social Cost	Travel Energy Cost (yuan/day)	Construction Cost (yuan/day)	Average Travel Time (min)	Total Travel Distance (km)	Computation Time (min)
High	[10, 30]	4604.77	9077.85	6561.95	18.12	1164.00	15.87
Medium	[30, 50]	5898.65	12370.29	7377.16	10.46	1131.43	14.53
Low	[50, 70]	7076.60	13107.60	11320.74	6.38	919.69	9.01

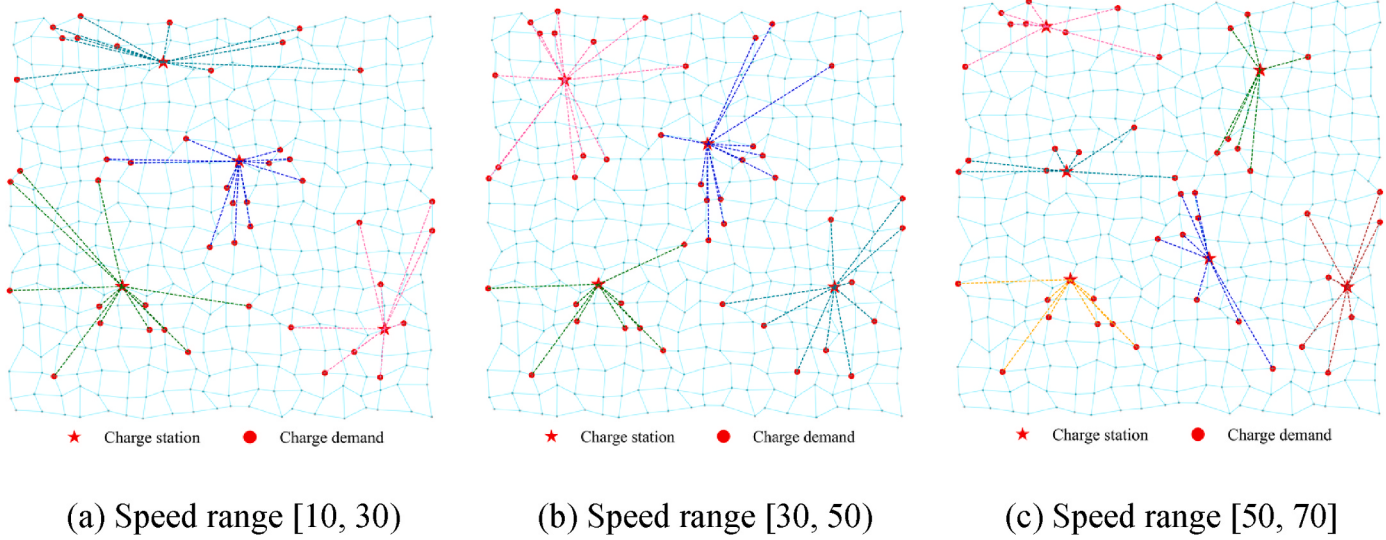


Fig. 9. Location results of ACECA under different levels of traffic volume.

### 5.3.3. Charging station capacity

The capacity of EVCS is jointly determined by site space availability and grid carrying capacity. In cases where space is sufficient, if the CS capacity is too large, there might be situations of insufficient power supply during peak EV charging periods, potentially affecting the supply-demand balance of electricity in the surrounding area. To prevent EV charging power from exceeding the maximum grid carrying capacity, it is necessary to constrain the charging capacity during the CS location selection stage. This paper provides model results for three different charging station capacities, as shown in Table 3 and Fig. 10.

From Table 3 and Fig. 10, it can be observed that for CS location selection schemes with lower grid capacities, the travel energy cost, travel time, and travel distance are lower compared to other scenarios, but the construction cost is higher. Although the CS location selection scheme with lower power grid capacity incurs construction costs that are 20.73 % and 32.13 % higher compared to the other two scenarios, the travel time and travel energy cost are at least 14.64 % and 6.08 % lower, respectively. This may be because the lower charging station capacity forces ACECA to select more clustering centers as charging stations to meet the necessary charging demand. Although an increase in the number of charging stations will result in higher construction costs, it will also shorten the travel distance and travel time for EVs to reach CS, thereby reducing travel energy cost. The shorter the travel time and distance, the more attractive CS is to EV users; the lower the EV travel energy cost, the higher the energy utilization rate, and the less additional economic cost for EV users need to pay. Therefore, it demonstrates

that a larger charging station capacity is not always better. While a smaller charging station capacity may increase the costs for operators, it also brings about better user experiences and environmental benefits. Thus, in the long term, larger charging station capacities will promote the generation of charging demand, thereby increasing the load on the city's grid.

### 5.4. Implication

Section 5.2 has demonstrated that the solution quality of ACECA is the best among the six algorithms, and its computational efficiency is outstanding. Based on the experimental results from Section 5.3, the applicable scenarios, economic aspects, and policy recommendations of the method proposed in this paper can be summarized as follows:

- The sensitivity of the algorithm's computational efficiency to the scales of road networks determines its application scenarios. ACECA exhibits shorter computation times on medium to small-scale road networks, but its computation time on large-scale road networks is not negligible and significantly increases with the expansion of the road network scale. However, this does not imply that the proposed method is only suitable for solving EVCS location selection problems in medium or small-scale cities, as the EVCS location selection problem prioritizes solution quality over solution time. Therefore, the proposed method has good applicability and strong portability in EVCS problems of various city

**Table 3**

Results under different charging station capacity constraints.

Power Grid Capacity	Charging Station Capacity	Total Social Cost	Travel Energy Cost (yuan/day)	Construction Cost (yuan/day)	Average Travel Time (min)	Total Travel Distance (km)	Computation Time (min)
Low	10	6960.65	13286.95	8610.61	11.73	1224.37	11.24
Medium	15	7008.62	15793.87	6825.83	13.89	1434.57	18.97
High	20	6264.37	14094.70	5844.20	13.45	1290.59	17.88

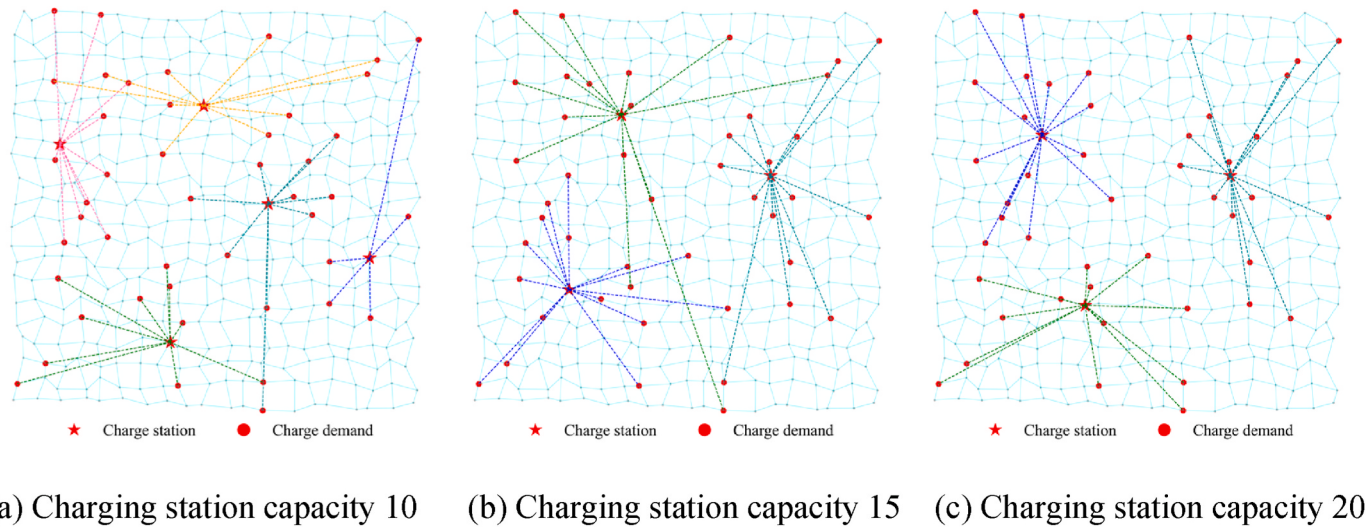


**Fig. 10.** Location results of ACECA under three different charging station capacities.

- scales but is not suitable for large-scale site planning problems with high time constraints.
- (ii) The level of traffic volume is an important influencing factor for CS location selection schemes and is closely related to the application scenarios, economic aspects, and environmental benefits of the proposed method. In road networks with high traffic volumes, the total social cost, travel energy cost, and construction cost of EVCS location selection solutions are lower than those with lower traffic volumes, which indicates a reduction in operator investment and energy wastage. However, higher traffic volumes also signify more congested traffic conditions, leading to increased travel time and detour distances for EVs to reach CS, thereby reducing charging convenience. This result suggests that applying the proposed method in cities with relatively congested traffic conditions can effectively enhance the economic and environmental benefits of EVCS but cannot improve the charging experience for EV users in congested traffic environments. Therefore, it is recommended for government departments to choose appropriate EVCS location selection planning methods based on the traffic operating conditions of the city, thereby achieving better economic and environmental benefits.
  - (iii) The capacity of charging stations influences the charging efficiency, economic and environmental benefits of location selection solutions. Under the premise of satisfying all charging demands, a smaller charging station capacity implies a greater number of required charging stations, leading to higher operator investment costs. While an increase in the number of charging stations will result in higher construction costs, it will also reduce travel energy costs, travel time, and travel distance, thereby enhancing the charging experience for EV users. Therefore, a larger charging station capacity indicates lower energy utilization rates, which will stimulate more charging demand, thereby increasing the load on the city's grid and posing challenges to urban sustainability. This conclusion suggests that governments should actively formulate capacity standards for EVCS construction to avoid energy wastage and ensure the economic and time costs of EV users' charging demands.

## 6. Conclusions

This study introduces a two-stage ACECA to solve the model for charging station location planning and electric vehicle charging paths. The research findings can be summarized as follows:

- (i) The number of proposed charging stations is a crucial factor influencing the optimization results of the model, and its range of values is closely related to the performance of the ACECA algorithm. Generally, the social cost of CS location plans exhibits a trend of initial decrease followed by an increase with the increase in the number of charging stations, indicating the presence of an optimal number of stations.
- (ii) Uncertainty in traffic environments can indirectly affect the optimization results of EV charging paths, which in turn can impact CS location plans. The ACECA demonstrates robustness with minimal variations in optimization results when uncertainty is introduced. Additionally, the optimized CS location plans generated by ACECA outperform those generated by other algorithms in terms of social cost and travel energy consumption, demonstrating significant advantages in energy conservation and pollution reduction.
- (iii) The proposed method can effectively enhance the economic and environmental benefits of EVCS location selection schemes in a congested traffic network, but it is unable to improve the charging convenience for EVs in this scenario.
- (iv) Increasing the capacity of charging stations can effectively reduce the construction cost investment for operators in CS location selection schemes, but it will also reduce the energy utilization rate, leading to more charging demand. Additionally, increasing the capacity of charging stations will also result in an increase in the travel distance and travel time for EVs to reach CS, thereby reducing the charging experience for EV users.

Although the proposed model and algorithm make a significant contribution to solving the CEOLRP, it is important to acknowledge that the study overlooks significant differences in economic development, population size, and policy aspects among countries. These factors are crucial in determining the scale and layout of charging stations. Furthermore, the congestion effect of transportation networks has not been fully considered in the model, which also affects the benefits of the EVCS location selection schemes. Future research should aim to develop more universally applicable mathematical models that consider various factors, such as economic development, population size, policies and congestion effect of transportation networks. Additionally, it is essential to develop algorithms with enhanced performance to provide valuable insights for optimizing decisions related to electric vehicle charging station layouts.

## CRediT authorship contribution statement

**Jiabin Wu:** Writing – original draft, Methodology, Funding acquisition, Conceptualization. **Qihang Li:** Visualization, Validation, Investigation, Data curation. **Yiming Bie:** Writing – review & editing, Supervision, Funding acquisition. **Wei Zhou:** Software, Formal analysis.

## Declaration of competing interest

The authors declare that they have no known competing financial interests or personal relationships that could have appeared to influence the work reported in this paper.

## Appendix A

### Appendix A

Main parameters and variables of the model.

Abbreviations	Definition		
EV	Electric vehicle	$\chi$	Vehicle frontal area
CS	Charging station	$P_{\text{char}}$	Rated power output of charging stations
EVCS	Electric vehicle charging station	$\lambda_1, \lambda_2, \lambda_3$	Coefficients of user capture degree, total travel cost, and total construction cost
LRP	Location-routing problem	$L_{\max}$	The maximum distance that EV users can accept when choosing a charging station
CEOLRP	Co-evolutionary optimization model of Location-routing problem	$S$	Set of states of charge, $s, s', s_m, s_n, SOC_{\min}, SOC_{\max} \in S$
ACECA	Adaptive co-evolutionary clustering algorithm	$P_{mn}$	The path with the shortest travel time of the EV from the demand point $m$ to the charging station point $n$ contains a number of nodes and arcs
IRSA	Improved ripple spreading algorithm	<b>Variables</b>	<b>Definition</b>
GA	Genetic algorithm	$x_n$	A binary decision variable for determining whether to construct a charging station at candidate location $n$ or not
IA	Immune algorithm	$y_{ij}$	A binary decision variable for determining whether an EV passes through road link $(i, j)$ or not
PSO	Particle swarm optimization	$T_{ijt}, T_{mnt}$	Travel time of EV from node $i$ ( $m$ ) to $j$ ( $n$ ) at time $t$
GWO	Grey wolf optimization	$e_{ijt}$	Energy consumption of EV from node $i$ to $j$ at time $t$
Parameters	Definition	$T_{mn}^{\text{char}}$	Charging time from EV's departure at demand point $m$ until charging to initial charge level at charging station $n$
$V, \bar{V}$	Set of nodes, $i, j, m, n \in V, (i, t, s), (j, t', s') \in \bar{V}$	$E_{mnt}$	Total energy consumption of EV traveling from demand point $m$ to CS $n$ at time $t$
$A, \bar{A}$	Set of arcs, $(i, j) \in A, (i, j, t, t', s, s') \in \bar{A}$	$a_{ijt}$	Free-flow travel time of arc $(i, j)$ at time $t$
$T$	Set of time intervals, $t, t', t'' \in T$	$Q_{ijt}$	Traffic on arc $(i, j)$ at time $t$
$M$	Set of EV charging demand points, $m \in M$	$C_{ijt}$	Capacity of arc $(i, j)$ at time $t$
$N$	Set of candidate CS locations, $n \in N$	$C_1$	Degree of user capture
$N_m, N_n$	The number of charging demand points and CSs	$C_2$	The cost of energy consumption for an EV traveling from the demand point to the charging station
$f_r$	Rolling coefficients of vehicles traveling through intersections	$C_3$	The total CS construction cost
$\beta, \gamma$	Parameters in the BPR function	$\eta_{mn}$	The number of EVs traveling from demand point $m$ to CS $n$
$\lambda$	Percentage of the motorized power to total braking power	$C_{mn}^{\text{char}}$	Charging fee incurred from EV's departure at demand point $m$ until charging to rated charge at CS $n$
$U$	The number of total braking time intervals under EV traveling conditions. The braking interval ordinal number $u \in U$	$\hat{T}_{ijt}$	Travel time budget of EV passing through road section $(i, j)$ at time $t$
$T_{\max}$	Parameters of isochrones for the service area of the charging station	$\mu_{ijt}, \sigma_{ijt}$	Mean and standard deviation of the travel time budget for EVs passing road segment $(i, j)$ at time $t$
$\kappa$	Charging price per unit of time	$\Phi^{-1}(\cdot)$	Inverse function of the standard normal distribution
$N_s$	The maximum number of EV charging stations planned for the region	$S_{mnt}, K_{mnt}$	Skewness and kurtosis of the total travel time $T_{mnt}$
$E_{\max}$	Rated capacity of EV battery	$\mu_{mnt}, \sigma_{mnt}$	Mean and variance of the total travel time of EV from demand point $m$ to CS $n$ at time $t$ and the distribution function it follows
$C_n^{\text{rent}}, C_n^{\text{build}}, C_n^{\text{oper}}$	Land lease cost, construction cost, operation and management cost for building charging station at node $n$	$\Omega(\cdot)$	The probability that the actual travel time taken by the EV along path $P_{mn}$ from demand point $m$ to CS $n$ at time $t$ is less than or equal to the travel time budget
$N_c, R$	The number of clustering centers and search radius of ACECA algorithm	$R_{mnt}$	The energy consumption of the road segment and the energy consumption at signalized intersection for EV traveling from demand point $m$ to CS $n$ at time $t$
$E_h^{\text{air}}, E_h$	Average air conditioning energy consumption per kilometer and per 100 km of EV at ambient temperature of $h$	$E_{\text{drive}}^{\text{mnt}}$	Energy consumption of EV traveling from demand point $m$ to CS $n$ at time $t$
$E_b, E_r$	Energy consumption and recovery generated during EV braking	$E_k(t_k)$	Energy consumption of EV passing through node $k$ at time $t_k$
$\eta_1, \eta_2$	Parameters of EV rolling resistance coefficient	$f_{ijt}^g$	Climbing resistance of EV through road section $(i, j)$
$W_d, W_a, W_e$	Power consumed by an EV to overcome resistance, acceleration, and the electrical equipment of the car's auxiliary devices while driving at node	$f_{ijt}, f_{ijt}^*, f_{ijt}^r$	Coefficients of combined force, traction force and rolling resistance of EV traveling on road section $(i, j)$ at time $t$
		$\bar{v}_{ijt}$	The space mean speed of the EV in the road section $(i, j)$ at time $t$

(continued on next page)

## Appendix A (continued)

$\eta_c$	Efficiency of the flywheel inertia to charge the battery via the electric motor	$\theta_{ij}$	Angle between road section $(i, j)$ and horizontal direction
$F_r, F_d, F_f$	Rolling resistance, air resistance, acceleration resistance of the EV	$f_{n1}, f_{n2}$	Degree of user capture when charging station is constructed at site $n$ and not constructed at site $n$
$\eta_{EV}$	Vehicle efficiency	$w_m, w_n$	Weights of EV demand point $m$ and charging station point $n$
$f_d, \rho$	Air resistance coefficient and air density	$L_{mn}$	Shortest path distance from EV demand point $m$ to charging station $n$
$v_t, v_b$	Vehicle travel speed at time $t$ , and in the braking state	$l_{ij}$	Length of the road segment $(i, j)$
$v'_u, v_u$	The final and initial speeds of the vehicle in the $u$ -th braking time interval	$\delta$	Rotating mass conversion factor

## References

- [1] Asamer J, Reinthaler M, Ruthmair M, Straub M, Puchinger J. Optimizing charging station locations for urban taxi providers. *Transp Res Pt A-Policy Pract* 2016;85: 233–46. <https://doi.org/10.1016/j.tra.2016.01.014>.
- [2] Han D, Ahn Y, Park S, Yeo H. Trajectory-interception based method for electric vehicle taxi charging station problem with real taxi data. *Int J Sustain Transp* 2016; 10:671–82. <https://doi.org/10.1080/15568318.2015.1104565>.
- [3] Zhang S, Wang H, Zhang Y, Li Y-Z. A novel two-stage location model of charging station considering dynamic distribution of electric taxis. *Sustain Cities Soc* 2019; 51:101752. <https://doi.org/10.1016/j.scs.2019.101752>.
- [4] He Y, Song Z, Liu Z. Fast-charging station deployment for battery electric bus systems considering electricity demand charges. *Sustain Cities Soc* 2019;48: 101530. <https://doi.org/10.1016/j.scs.2019.101530>.
- [5] Ferro G, Minciardi R, Robba M. A user equilibrium model for electric vehicles: joint traffic and energy demand assignment. *Energy* 2020;198:117299. <https://doi.org/10.1016/j.energy.2020.117299>.
- [6] Liu K, Liu Y. Stochastic user equilibrium based spatial-temporal distribution prediction of electric vehicle charging load. *Appl Energy* 2023;339:120943. <https://doi.org/10.1016/j.apenergy.2023.120943>.
- [7] Chen Z, Deng Y, Xie C, et al. Network equilibrium of battery electric vehicles considering drivers' resting behavior. *Transport Res C Emerg Technol* 2023;155: 104305. <https://doi.org/10.1016/j.trc.2023.104305>.
- [8] Zhang J, Yan J, Liu YQ, et al. Daily electric vehicle charging load profiles considering demographics of vehicle users. *Appl Energy* 2020;274. <https://doi.org/10.1016/j.apenergy.2020.115063>.
- [9] Guo SL, Li PP, Ma K, et al. Robust energy management for industrial microgrid considering charging and discharging pressure of electric vehicles. *Appl Energy* 2022;325. <https://doi.org/10.1016/j.apenergy.2022.119846>.
- [10] Zhao Y, Wang ZP, Shen ZJM, et al. Data-driven framework for large-scale prediction of charging energy in electric vehicles. *Appl Energy* 2021;282. <https://doi.org/10.1016/j.apenergy.2020.116175>.
- [11] Li T, Ge Y, Xiong J, et al. Ridesharing user equilibrium model without the enroute transfer: an OD-based link-node formulation. *Transport Res E Logist Transport Rev* 2024;187:103599. <https://doi.org/10.1016/j.tre.2024.103599>.
- [12] Chen X, Di X. Ridesharing user equilibrium with nodal matching cost and its implications for congestion tolling and platform pricing. *Transport Res C Emerg Technol* 2021;129:103233. <https://doi.org/10.1016/j.trc.2021.103233>.
- [13] Huang R, Han Lee D, Huang Z. A new network equilibrium flow model: user-equilibrium with quantity adjustment. *Transport Res E Logist Transport Rev* 2022; 163:102719. <https://doi.org/10.1016/j.tre.2022.102719>.
- [14] Ma J, Meng Q, Cheng L, et al. General stochastic ridesharing user equilibrium problem with elastic demand. *Transp Res Part B Methodol* 2022;162:162–94. <https://doi.org/10.1016/j.trb.2022.06.001>.
- [15] Guo F, Yang J, Lu J. The battery charging station location problem: impact of users' range anxiety and distance convenience. *Transp Res Pt E-Logist Transp Rev* 2018; 114:1–18. <https://doi.org/10.1016/j.tre.2018.03.014>.
- [16] Hu D, Huang L, Liu C, Liu Z, Ge M. Data driven optimization for electric vehicle charging station locating and sizing with charging satisfaction consideration in urban areas. *IET Renew Power Gener* 2022;16:2630–43. <https://doi.org/10.1049/rpg2.12382>.
- [17] Erbaş M, Kabak M, Özçaylan E, Çetinkaya C. Optimal siting of electric vehicle charging stations: a GIS-based fuzzy Multi-Criteria Decision Analysis. *Energy* 2018; 163:1017–31. <https://doi.org/10.1016/j.energy.2018.08.140>.
- [18] Liu J, Zhang T, Zhu J, Ma T. Allocation optimization of electric vehicle charging station (EVCS) considering with charging satisfaction and distributed renewables integration. *Energy* 2018;164:560–74. <https://doi.org/10.1016/j.energy.2018.09.028>.
- [19] Panah PG, Bornapour SM, Nosratabadi SM, Guerrero JM. Hesitant fuzzy for conflicting criteria in multi-objective deployment of electric vehicle charging stations. *Sustain Cities Soc* 2022;85:104054. <https://doi.org/10.1016/j.scs.2022.104054>.
- [20] Guler D, Yomralioğlu T. Suitable location selection for the electric vehicle fast charging station with AHP and fuzzy AHP methods using GIS. *Spatial Sci* 2020;26: 169–89. <https://doi.org/10.1080/19475683.2020.1737226>.
- [21] Rani P, Mishra AR. Fermatean fuzzy Einstein aggregation operators-based MULTIMOORA method for electric vehicle charging station selection. *Expert Syst Appl* 2021;182:115267. <https://doi.org/10.1016/j.eswa.2021.115267>.
- [22] Zhou G, Dong Q, Zhao Y, et al. Bilevel optimization approach to fast charging station planning in electrified transportation networks. *Appl Energy* 2023;350: 121718. <https://doi.org/10.1016/j.apenergy.2023.121718>.
- [23] Song M, Cheng L, Zhang Y. Joint location optimization of charging stations and segments in the space-time-electricity network: an augmented Lagrangian relaxation and ADMM-based decomposition scheme. *Comput Ind Eng* 2023;183: 109517. <https://doi.org/10.1016/j.cie.2023.109517>.
- [24] Wang Y, Zhao Y, Gan S, et al. Optimization of charging stations integrated with dynamic transportation systems in metropolises. *Transport Res Transport Environ* 2023;119:103726. <https://doi.org/10.1016/j.trd.2023.103726>.
- [25] Zhou G, Zhu Z, Luo S. Location optimization of electric vehicle charging stations: based on cost model and genetic algorithm. *Energy* 2022;247:123437. <https://doi.org/10.1016/j.energy.2022.123437>.
- [26] He SY, Kuo Y-H, Sun KK. The spatial planning of public electric vehicle charging infrastructure in a high-density city using a contextualised location-allocation model. *Transp Res Pt A-Policy Pract* 2022;160:21–44. <https://doi.org/10.1016/j.tra.2022.02.012>.
- [27] Ren X, Zhang H, Hu R, Qiu Y. Location of electric vehicle charging stations: a perspective using the grey decision-making model. *Energy* 2019;173:548–53. <https://doi.org/10.1016/j.energy.2019.02.015>.
- [28] Hosseini S, Sarder M. Development of a Bayesian network model for optimal site selection of electric vehicle charging station. *Int J Electr Power Energy Syst* 2019; 105:110–22. <https://doi.org/10.1016/j.ijepes.2018.08.011>.
- [29] Li C, Zhang L, Ou Z, Wang Q, Zhou D, Ma J. Robust model of electric vehicle charging station location considering renewable energy and storage equipment. *Energy* 2022;238:121713. <https://doi.org/10.1016/j.energy.2021.121713>.
- [30] Li J, Liu C, Wang Y, Chen R, Xu X. Bi-level programming model approach for electric vehicle charging stations considering user charging costs. *Elec Power Syst Res* 2023;214:108889. <https://doi.org/10.1016/j.epsr.2022.108889>.
- [31] Li Y, Su S, Liu B, Yamashita K, Li Y, Du L. Trajectory-driven planning of electric taxi charging stations based on cumulative prospect theory. *Sustain Cities Soc* 2022;86: 104125. <https://doi.org/10.1016/j.scs.2022.104125>.
- [32] Qiao D, Wang G, Xu M. Fast-charging station location problem: a two-phase approach with mathematical program with equilibrium constraints considering charging choice behaviour. *Sustain Cities Soc* 2023;96:104678. <https://doi.org/10.1016/j.scs.2023.104678>.
- [33] Song M, Cheng L, Du M, Sun C, Ma J, Ge H. Charging station location problem for maximizing the space-time-electricity accessibility: a Lagrangian relaxation-based decomposition scheme. *Expert Syst Appl* 2023;222:119801. <https://doi.org/10.1016/j.eswa.2023.119801>.
- [34] Ji J, Bie Y, Wang L. Optimal electric bus fleet scheduling for a route with charging facility sharing. *Transport Res C Emerg Technol* 2023;147:104010. <https://doi.org/10.1016/j.trc.2022.104010>.
- [35] Ezaki T, Imura N, Nishinari K. Towards understanding network topology and robustness of logistics systems. *Communications in Transportation Research* 2022; 2:100064. <https://doi.org/10.1016/j.comctr.2022.100064>.
- [36] Ruan T, Lv Q. Public perception of electric vehicles on reddit over the past decade. *Communications in Transportation Research* 2022;2:100070. <https://doi.org/10.1016/j.comctr.2022.100070>.
- [37] Li J, Liu Z, Wang X. Public charging station localization and route planning of electric vehicles considering the operational strategy: a bi-level optimizing approach. *Sustain Cities Soc* 2022;87:104153. <https://doi.org/10.1016/j.scs.2022.104153>.
- [38] Jordán J, Palanca J, Val E, et al. Localization of charging stations for electric vehicles using genetic algorithms. *Neurocomputing* 2021;452:416–23. <https://doi.org/10.1016/j.neucom.2019.11.122>.
- [39] Li J, Liu Z, Wang X. Public charging station location determination for electric ride-hailing vehicles based on an improved genetic algorithm. *Sustain Cities Soc* 2021; 74:103181. <https://doi.org/10.1016/j.scs.2021.103181>.
- [40] Wang Y, Liu D, Wu Y, Xue H, Mi Y. Locating and sizing of charging station based on neighborhood mutation immune clonal selection algorithm. *Elec Power Syst Res* 2023;215:109013. <https://doi.org/10.1016/j.epsr.2022.109013>.
- [41] Altudogun TG, Yildiz A, Karakose E. Genetic algorithm approach based on graph theory for location optimization of electric vehicle charging stations. In: *2021 Innovations in intelligent systems and applications Conference. ASYU*; 2021. p. 1–5.
- [42] Song M, Cheng L, Ge H, Li Y, Sun C. A stabilizing benders decomposition method for the accessibility-oriented charging station location problem. *Sustain Cities Soc* 2023;94:104558. <https://doi.org/10.1016/j.scs.2023.104558>.

- [43] Wei G, Lei F, Lin R, Wang R, Wei Y, Wu J, et al. Algorithms for probabilistic uncertain linguistic multiple attribute group decision making based on the GRA and CRITIC method: application to location planning of electric vehicle charging stations. *Econ Res-Ekon Istraz* 2020;33:828–46. <https://doi.org/10.1080/1331677X.2020.1734851>.
- [44] Zhao Z, Lee CKM, Huo J. EV charging station deployment on coupled transportation and power distribution networks via reinforcement learning. *Energy* 2023;267:126555. <https://doi.org/10.1016/j.energy.2022.126555>.
- [45] Li Y, Wang J, Wang W, Liu C, Li Y. Dynamic pricing based electric vehicle charging station location strategy using reinforcement learning. *Energy* 2023;281:128284. <https://doi.org/10.1016/j.energy.2023.128284>.
- [46] Lien JW, Mazalov VV, Melnik AV, Zheng J. Wardrop equilibrium for networks with the BPR latency function. In: 9th international conference on discrete optimization and operations research. DOOR; 2016. p. 37–49.
- [47] Xu X, Chen A, Cheng L, Lo HK. Modeling distribution tail in network performance assessment: a mean-excess total travel time risk measure and analytical estimation method. *Transp Res Part B Methodol* 2014;66:32–49. <https://doi.org/10.1016/j.trb.2013.09.011>.
- [48] Ge X, He H, Fu Y, Li Y, Xia S. Interchange and charging path planning of shared electric vehicles based on A\* algorithm combined with hierarchical programming. *Proceedings of the CSEE* 2021;41:7668–80. <https://doi.org/10.13334/j.0258-8013.pcsee.201409>.
- [49] Zhang Z, Wang J, Feng X, Chang L, Chen Y, Wang X. The solutions to electric vehicle air conditioning systems: a review. *Renew Sustain Energy Rev* 2018;91:443–63. <https://doi.org/10.1016/j.rser.2018.04.005>.
- [50] Hu L, Zhou D, Huang J, Du R, Zhang X. Optimal path planning for electric vehicle with consideration of traffic light and energy consumption. *Automot Eng* 2021;43:641–66. <https://doi.org/10.19562/j.chinasae.qcgc.2021.05.001>.
- [51] Wu J, He J, Lin Y, Bie Y. Co-evolutionary location-routing model of medical isolation areas for major public health emergencies considering the uncertainty of future traffic environment. *Transport Res Rec* 2023;2677:1408–23. <https://doi.org/10.1177/03611981221124591>.
- [52] Hu X-B, Zhang M-K, Zhang Q, Liao J-Q. Co-Evolutionary path optimization by Ripple-Spreading algorithm. *Transp Res Part B Methodol* 2017;106:411–32. <https://doi.org/10.1016/j.trb.2017.06.007>.
- [53] Hu X-B, Wang M, Leeson MS, Di Paolo EA, Liu H. Deterministic agent-based path optimization by mimicking the spreading of ripples. *Evol Comput* 2016;24:319–46. [https://doi.org/10.1162/EVCO\\_a\\_00156](https://doi.org/10.1162/EVCO_a_00156).
- [54] Dan M, Ban X, Jeff. Optimal locations and sizes of layover charging stations for electric buses. *Transport Res C Emerg Technol* 2023;152:104157. <https://doi.org/10.1016/j.trc.2023.104157>.
- [55] Ji J, Bie Y, Shi H, et al. Energy-saving speed profile planning for a connected and automated electric bus considering motor characteristic. *J Clean Prod* 2024;448:14172. <https://doi.org/10.1016/j.jclepro.2024.141721>.